IWB

Modelling Corrosion of Steel Reinforcement in Concrete – Fully Coupled 3D FE Model

J. Ožbolt[1,2]

G. Balabanić[2], M. Kušter[3] & F. Oršanić[1]

[1]University of Stuttgart, Institute of Construction Materials, Germany
[2]University of Rijeka, Faculty of Civil Engineering, Croatia
[3]University of Zagreb, Faculty of Civil Engineering, Croatia

Supported by National Science Foundations of Germany & Croatia

Aix-en-Provence, France
May 29-June 1, 2012

Outline

- Introduction & motivation
- Modeling of processes before and after depassivation of steel reinforcement (chloride induced corrosion)
- Chemo-hygro-thermo-mechanical model for concrete
- Numerical example (1) – processes before depassivation
- Numerical example (2) – processes after depassivation
- Summary and conclusions

Introduction & motivation

- Corrosion of reinforcement - one of the major causes of deterioration of reinforced concrete (RC) structures
- Consequences:
  - reduction of steel cross-section area
  - damage of concrete cover due to expansion of corrosion product
  - decrease of ductility of steel (pitting effect)
  - degradation of bond resistance (spalling)
- Reliable 3D numerical model useful for:
  - prediction of service life of RC structures (new & existing structures)
  - formulation of simple engineering models & design rules

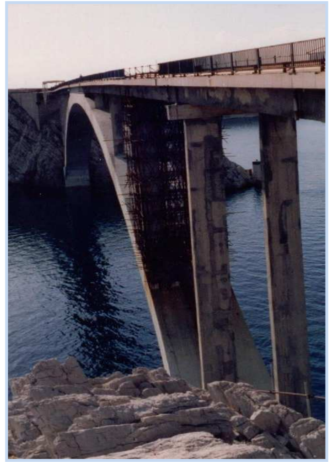

Processes to be modeled

- Non-mechanical processes:
  - Transport of capillary water, heat, oxygen and chloride through the concrete cover
  - Immobilization of chloride in the concrete
  - Chathodic and anodic polarization
  - Transport of OH^- ions through electrolyte in concrete pores
  - Calculation of corrosion rate, current density and electrical potential
  - Transport of corrosion products (rust)
- Mechanical processes:
  - Corrosion induced damage and cracking of concrete
- Interaction between mechanical and non-mechanical processes

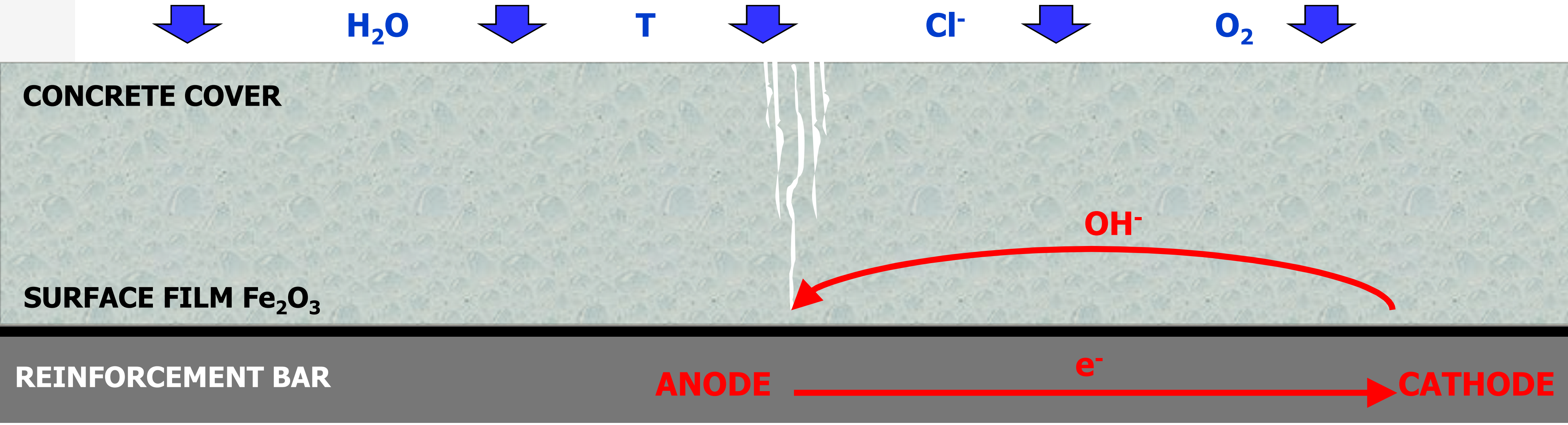

IWB

Theoretical framework

- Continuum mechanics
  - Green-Lagrange strain tensor
  - Co-rotational stress tensor
- Irreversible thermodynamics
- Mechanical model - microplane model for concrete based on the relaxed kinematic constraint
- Discretization method - standard finite elements
- Smeared crack concept with crack band method as a localization limiter

Depassivation of reinforcement

- Dissolution of iron at the anodic sites (anodic half-cell)

$$2Fe \rightarrow 2Fe^{2+} + 4e^-$$

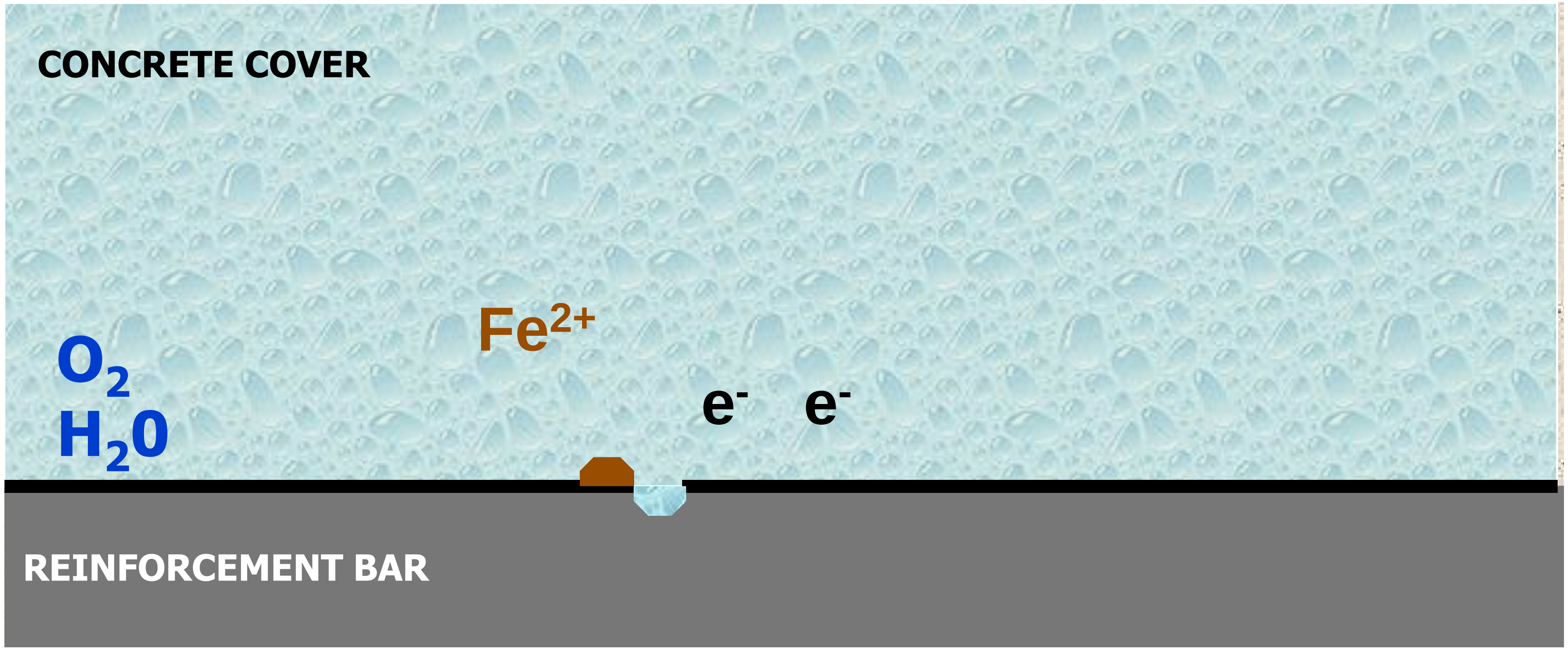

After depasivation of reinforcement

- Reaction of dissolved oxygen in the pore water with the electrons on the cathode (cathodic half-cell)

$$2H_2O + O_2 + 4e^- \rightarrow 4OH^-$$

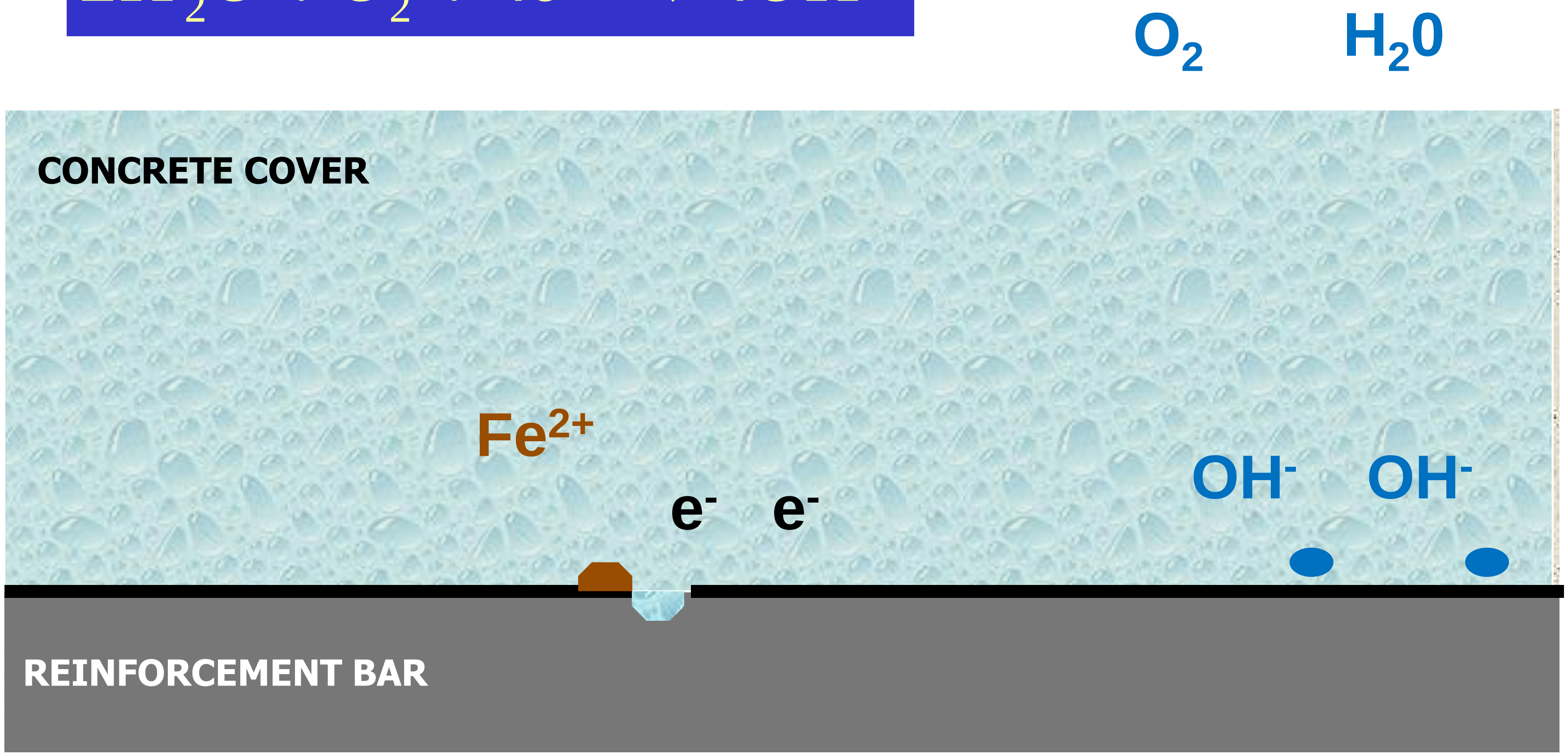

After depasivation of reinforcement

- Transport of hydroxyl ions to the anode, where corrosion products are formed

$$Fe^{2+} + 2OH^{-} \rightarrow Fe(OH)_2$$

$$4Fe(OH)_2 + O_2 + 2H_2O \rightarrow 4Fe(OH)_3$$

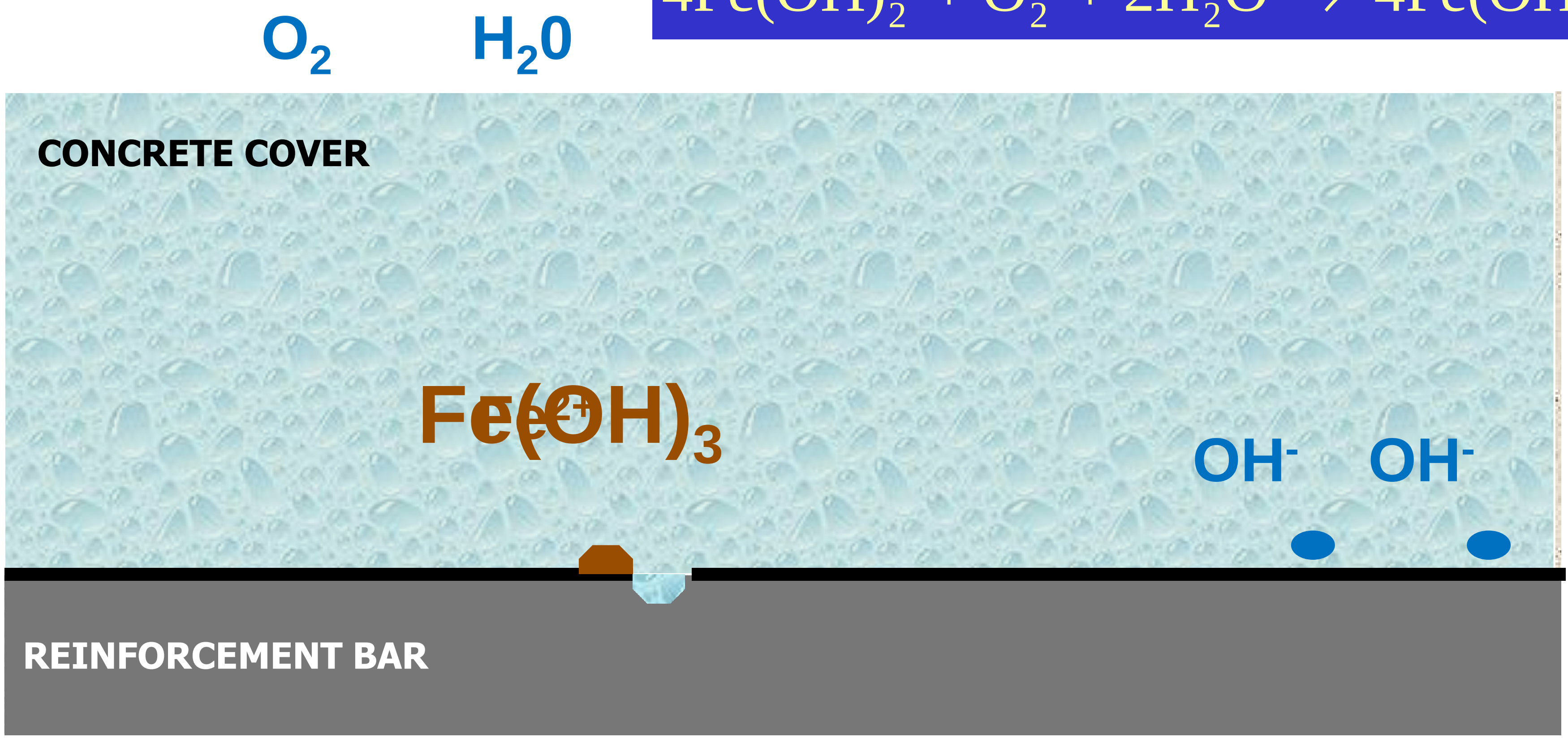

Mathematical description of non-mechanical processes before depassivation of steel

Transport of capilary water θ_w (m^3 of water / m^3 of concrete):

$$\frac{\partial \theta_w}{\partial t} = \nabla \cdot [D_w(\theta_w)\nabla \theta_w]$$

Transport of oxigen C_o (kg of oxygen / m^3 of pore solution):

$$\theta_w \frac{\partial C_o}{\partial t} = \nabla \cdot [\theta_w D_o(\theta_w)\nabla C_o] + D_w(\theta_w)\nabla \theta_w \nabla C_o$$

Transport of free chlorides ions C_c (kgCl - /m^3 pore solution):

$$\theta_w \frac{\partial C_c}{\partial t} = \nabla \cdot [\theta_w D_c(\theta_w, T)\nabla C_c] + D_w(\theta_w)\nabla \theta_w \nabla C_c - \frac{W_{gel}}{1000} \cdot \frac{\partial C_{cb}}{\partial t}$$

Transport of bound chlorides ions C_{cb} (gCl$^-$ / kg$_{gel}$):

$$\frac{\partial C_{cb}}{\partial t} = k_r \left(\alpha C_c^{\beta} - C_{cb}\right)$$

Transport heat W (W / m^3):

$$\lambda \Delta T + W(T) - c\rho \frac{\partial T}{\partial t} = 0$$

References:

Bažant and Najjar, 1971
Bear and Bachmat, 1991
Balabanić et al., 1996
Martín – Pérez, 1999
Tang and Nillson, 1996a, 1996b
Isgor and Razaqpur, 2006
Ožbolt et al., 2010

Numerical implementation - transient FE analysis
(before depassivation)

Non-mechanical part: direct integration of implicit type (iterative solution)

$$\left[P_{\theta_w}\right]\left\{\dot{\theta}_w\right\}+\left[K_{\theta_w}\right]\left\{\theta_w\right\}=\{0\}$$

$$\left[P_{C_o}\right]\left\{\dot{C}_o\right\}+\left[K_{C_o}\right]\left\{C_o\right\}=\{0\}$$

$$\left[P1_{C_c}\right]\left\{\dot{C}_c\right\}+\left[P1_{C_{cb}}\right]\left\{\dot{C}_{cb}\right\}+\left[K_{C_c}\right]\left\{C_c\right\}=\{0\}$$

$$\left[P2_{C_{cb}}\right]\left\{\dot{C}_{cb}\right\}+\left[P2_{C_c}\right]\left\{\dot{C}_c\right\}+\left[P3_{C_{cb}}\right]\left\{C_{cb}\right\}=\{0\}$$

$$\left[C_T\right]\left\{\dot{T}\right\}+\left(\left[K\right]+\left[H\right]\right)\left\{T\right\}=\left\{R\right\}$$

with:

$$\left[P_{\theta_w}\right]=\int_\Omega [N]^T[N]d\Omega \quad [K\theta_w]=\int_{½} D_w(\theta_w)[\nabla N]^T[\nabla N]d½ \quad \left[P_{C_0}\right]=\int_\Omega \theta_w[N]^T[N]d\Omega$$

$$\left[K_{C_0}\right]=\int_\Omega \theta_w D_o(\theta_w)[\nabla N]^T[\nabla N]d\Omega-\int_\Omega D_w(\theta_w)\nabla\theta_w[N]^T[N]d\Omega$$

$$\left[P1_{C_0}\right]=\int_\Omega \theta_w[N]^T[N]d\Omega \quad \left[P2_{C_c}\right]=\int_\Omega k_r\alpha[N]^T[N]d\Omega$$

$$\left[K_{C_c}\right]=\int_\Omega \theta_w D_c(\theta_w,T)[\nabla N]^T[\nabla N]d\Omega-\int_\Omega D_w(\theta_w)\nabla\theta_w[N]^T[N]d\Omega$$

$$\left[P1_{C_{cb}}\right]=\int_\Omega W_{gel}\cdot 10^{-3}[N]^T[N]d\Omega \quad \left[P2_{C_{cb}}\right]=\int_\Omega -[N]^T[N]d\Omega$$

$$\left[P3_{C_{cb}}\right]=\int_\Omega -k_r[N]^T[N]d\Omega \quad [C_T]=\int_\Omega c\rho[N]^T[N]d\Omega \quad [K]=\int_\Omega \lambda[\nabla N]^T[\nabla N]d\Omega$$

$$[H]=\int_\Gamma \alpha_{TR}[N]^T[N]d\Gamma \quad [R]=\int_\Omega W(T)[N]^T d\Omega+\int_\Gamma \alpha_{TR}[N]^T T_M d\Gamma$$

Mechanical part: secant-stiffness approach with Newthon-Rapshon iteration

$$[K_m]\{\dot{u}\}=\{\mathrm{f}\}$$

with:

$$[K_m]=\int_\Omega \left[\frac{\partial N}{\partial \mathbf{x}}\right]^T [D_m]\left[\frac{\partial N}{\partial \mathbf{x}}\right]d\Omega;$$

Mathematical description of non-mechanical processes after depassivation of steel

STRONG FORM

Transport of oxygen: $\frac{\partial C_o}{\partial t} = D_o(S_w, p_{con})\nabla^2 C_o + D_w(\theta_w)\nabla\theta_w\nabla C_o$

Electric potential (conservation of electric charge): $\nabla^2\Phi = 0$

Current density:

$\mathbf{i} = -\sigma(S_w, p_{con})\nabla\Phi$

Oxygen consumption: $D_o(S_w, p_{con})\left.\frac{\partial C_o}{\partial n}\right|_{anode} = -k_a i_a$ $\quad D_o(S_w, p_{con})\left.\frac{\partial C_o}{\partial n}\right|_{cathode} = -k_c i_c$

Polarization:
(Butler – Volmer kinetics)

$Anode: \Phi = \Phi_{0a} + \frac{\beta_c}{2.3}\ln\left(\frac{i_a}{i_{0a}}\right)$ $\quad Chatode: \Phi = \Phi_{0c} - \frac{\beta_c}{2.3}\ln\left(\frac{i_c}{i_{0c}}\cdot\frac{C_{ob}}{C_o}\right)$

WEAK FORM (finite elements): direct integration of implicit type (iterative solution)

$$[A_o]\{C_o\} + [B_o]\left\{\frac{\partial C_o}{\partial t}\right\} = \{f_o\}$$

$$[A_\Phi]\{\Phi\} = \{0\}$$

with:

$[A_o] = D_o(S_w, p_{con})\int_\Omega [\nabla N]^T [\nabla N] d\Omega \quad , \quad [B_o] = \int_\Omega [N]^T [N] d\Omega$

$\{f_o\} = -k_a i_a \int_\Gamma N d\Gamma$ at anodic surface

$\{f_o\} = -k_c i_c \int_\Gamma N d\Gamma$ at cathodic surface

$[A_\Phi] = \int_\Omega [\nabla N]^T [\nabla N] d\Omega$

Ožbolt et al., 2011

Mathematical description of non-mechanical processes after depassivation of steel

Expansion of corrosion product:

$$J_r = 5.536\times10^{-7}\, i_a$$

$$m_r = J_r \Delta t A_r$$

J_r = Rate of rust production (kg/m^{2}s)
m_r = Mass of hydrated rust per unit length of rebar (kg/m)
A_r = Corresponding surface of reinforcement (m^2)
Δt = Time increment

$$\Delta l_r = \frac{m_r}{A_r}\left(\frac{1}{\rho_r} - \frac{0.523}{\rho_s}\right)$$

Δl_r = Radial expansion of of corrosion product (m)
ρ_r = 1.96×10^3 (kg/m^3)
ρ_s = 7.89×10^3 (kg/m^3)

Transport of corrosion products through pores and cracks:

$$\theta_w \frac{\partial R}{\partial t} = \nabla\cdot\left[\theta_w D_r \nabla R\right] + D_w(\theta_w)\nabla\theta_w \nabla R$$

R = Rust (kg/m^3 of pores solution)
D_r = Diffusion coefficient of rust (m^2/s)

Transport of rust through cracks

Chemo-hygro-thermo-mechanical coupling

Decomposition of strain (index notation):

$$\varepsilon_{ij} = \varepsilon_{ij}^{m} + \varepsilon_{ij}^{T} + \varepsilon_{ij}^{w} + \varepsilon_{ij}^{corr}; \quad \varepsilon_{ij}^{m} = \varepsilon_{ij} - (\varepsilon_{ij}^{T} + \varepsilon_{ij}^{w} + \varepsilon_{ij}^{corr})$$

with:

ε_{ij}^{m} = mechanical strain

ε_{ij}^{T} = non-elasic strain due to temperature

ε_{ij}^{w} = non-elasic strain due to wetting drying of concrete

ε_{ij}^{corr} = non-elasic strain due to corrosion of steel-concrete interface

Equlilibrium:

$$\frac{\partial \sigma_{ij}^{m}(\varepsilon_{ij}^{m}, \theta_{w}, T)}{\partial X_{i}} + \rho g_{i} = 0$$

Constitutive law: temperature & humidity dependent microplane model

Thermo-hygro dependent microplane model for concrete

(co-rotational stress tensor, GL-strain tensor)

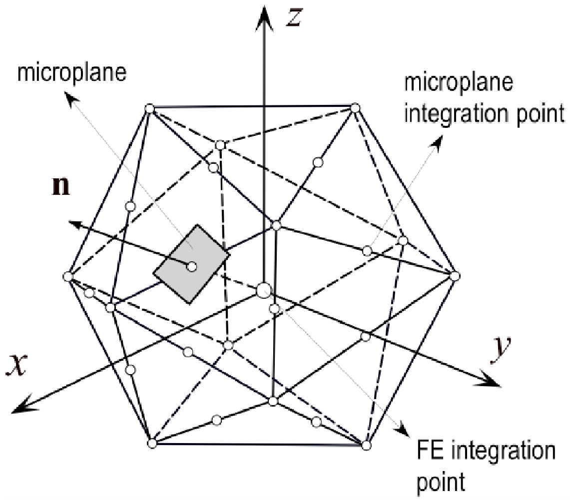

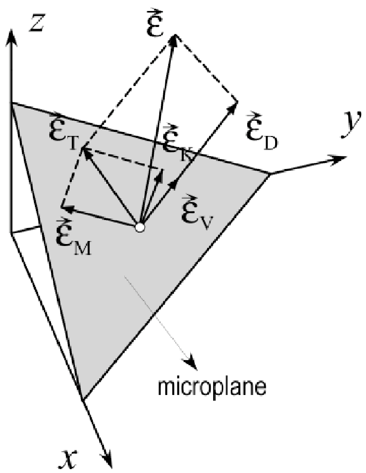

$$\sigma_{ij}^{m} = \sigma_V \delta_{ij} + \frac{3}{2\pi} \int_S \sigma_D (n_i n_j - \frac{\delta_{ij}}{3}) dS + \frac{3}{2\pi} \int_S \frac{\sigma_{Tr}}{2} (n_i \delta_{rj} + n_j \delta_{ri}) dS$$

Coupling: mechanical & non-mechanical parts of the model

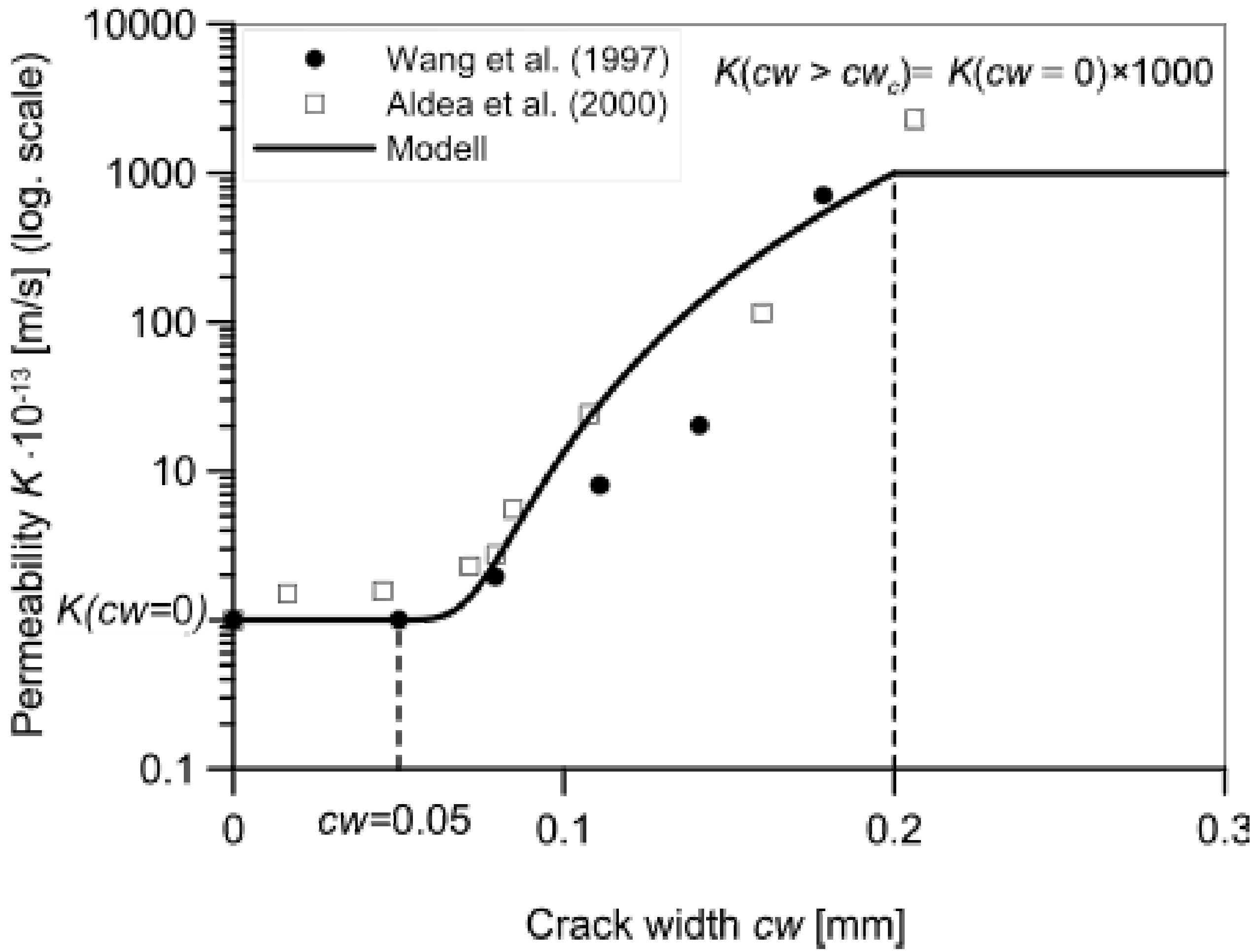

Assumption: diffusivity (D) & permeability (K) - function of the crack width

Discrete contact elements at the surface of reinforcement bar in radial (normal) and axial (shear) directions

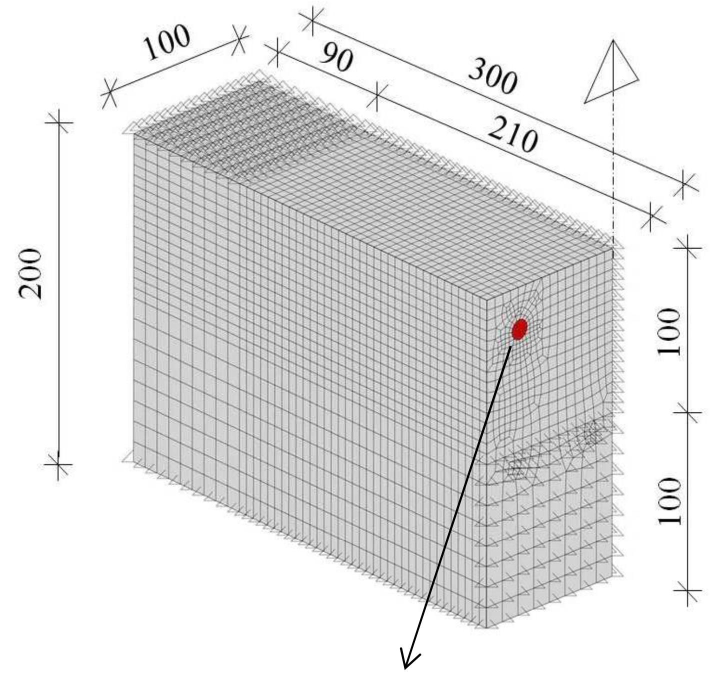

Corroded steel reinforcement

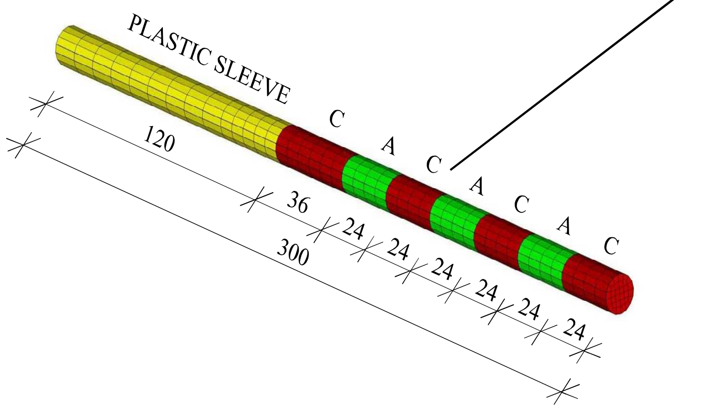

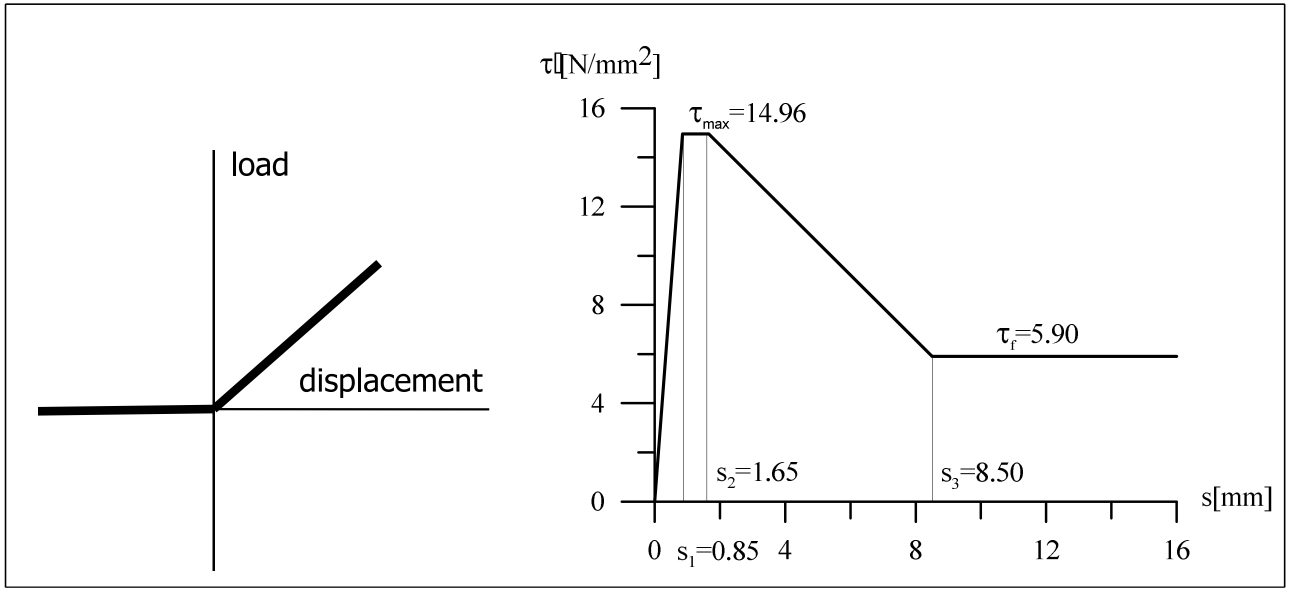

Radial and Tangential contact elements (bond) on the surface of corroded reinforcement

Numerical algorithm

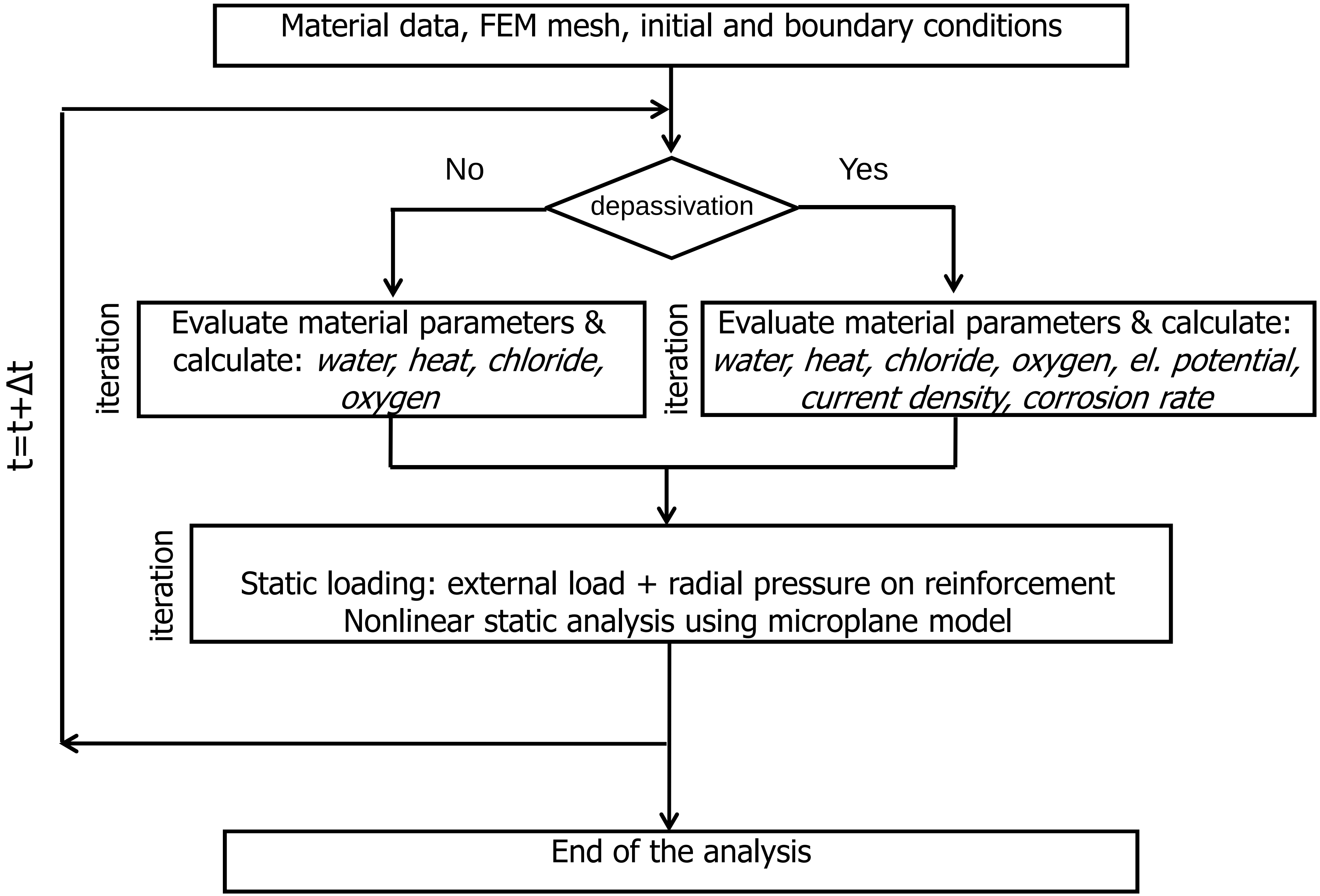

IWB

Numerical example (1)
(before depassivation of reinforcement)

Summary of material parameters

Modulus of elasticity of concrete, E_c (MPa):	25000
Modulus of elasticity of steel, E_s (MPa):	200000
Poisson's ratio:	0.18
Tensile strength, f_t (MPa):	2.0
Uniaxial compressive strength, f_c (MPa) :	25.0
Fracture energy, G_F (J/m^2):	80.0
Thermal conductivity, λ (W/mK):	2.1
Heat capacity per unit mass, c (J/kgK):	900
Mass density of concrete, ρ (kg/m^3):	2300
Limiting value of capillary water diffusivity, D_0 (m^2/s):	2.2E-10
Water volume in concrete at saturation, θ_{wd} (m^3/m^3):	0.1
Initial concrete porosity, p_c:	0.1
Aggregate/Cement ratio, a/c:	6.5
Water/Cement ratio, w/c:	0.5
Density of cement, ρ_c (kg/m^3):	3000
Density of aggregate, ρ_a (kg/m^3):	2650
Density of water, ρ_w (kg/m^3):	1000
Amount of cement gel in concrete, W_{gel} (kg/m^3):	400
Equivalent hydratation time period, t_e (days):	180
Reference chloride diffusion coefficient (m^2/s):	5.5E-12
Chloride binding rate coefficient (s^{-1}):	1.0E-05
α	3.57
β	0.38
Universal gas constant, R (kJ/molK):	8.31E-03
Chloride diffusion activation energy, U (kJ/mol):	44.6

RC slab

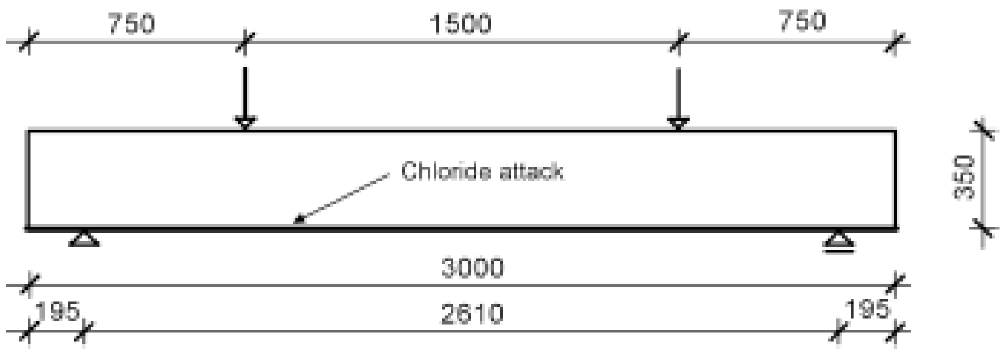

Loading history:

- Mechanical load (yielding of reinforcement)
- Chloride attack at the bottom side of the slab

Ozbolt et al., 2010

Distribution of damage

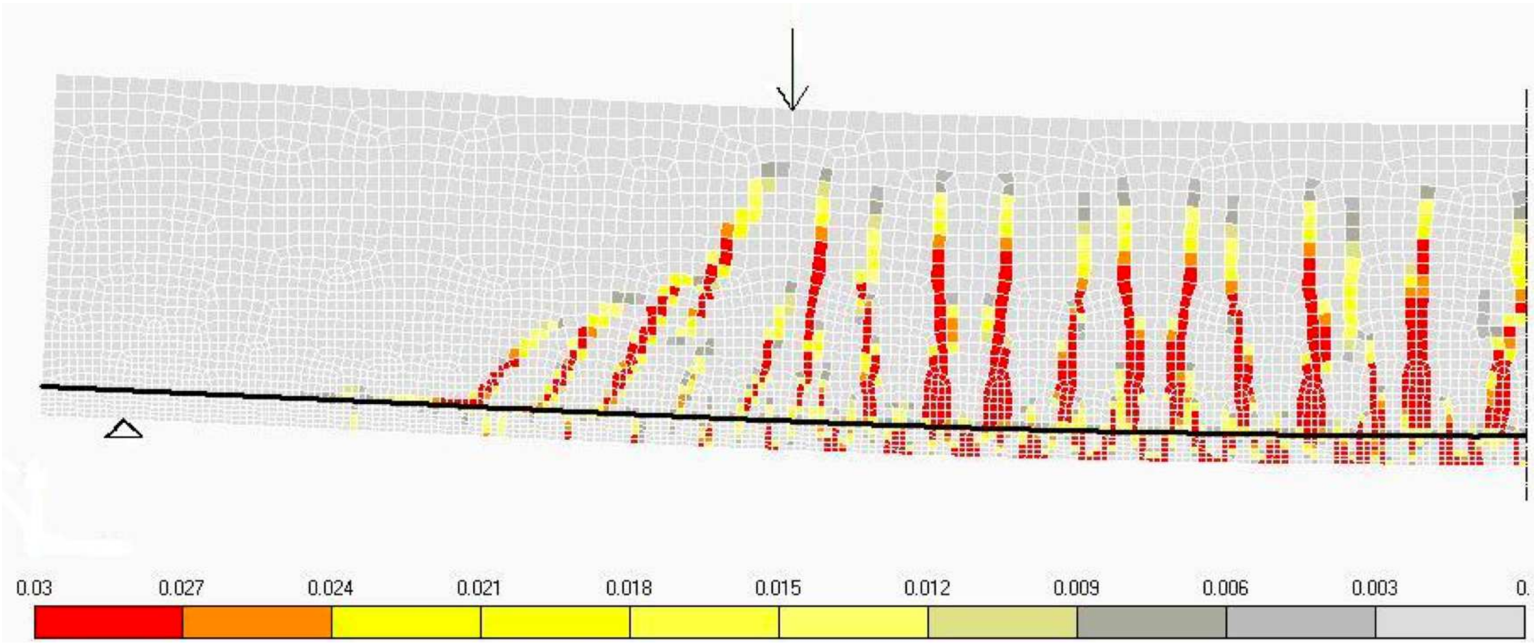

Distribution of water and oxygen

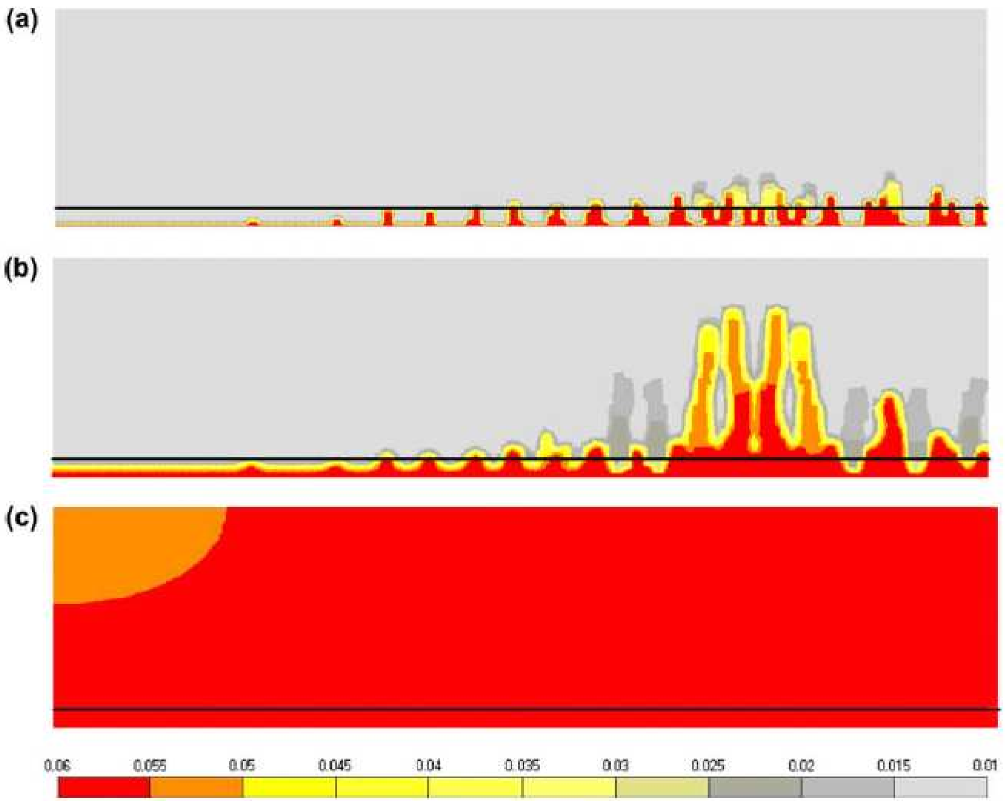

Distribution of water over the section of the slab after: 1 hour, 1 day and 1 year when the maximum value is reached along the entire height

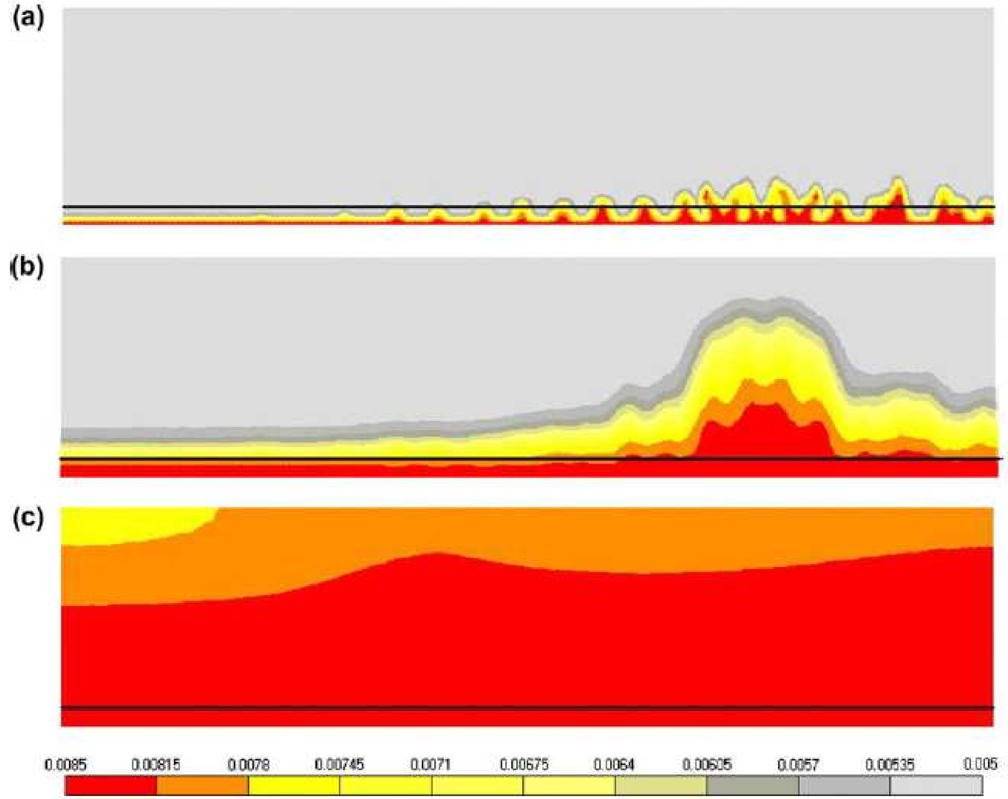

Distribution of oxygen (kg/m^3 of pore solution) over the section of the slab after: 1 hour, 1 day and 2 months when the maximum value is reached along the entire height

- Immediately after crack opening water, oxygen and free chlorides penetrate into the crack
- In good agreement with experimental observation (Wittmann et al. 2009; Marsavina et al. 2008)

IWB

Distribution of free and bond chlorides after 1 hour, 1 day, 1 year & 10 years

(red = 10 kg/m^3 of pore solution)

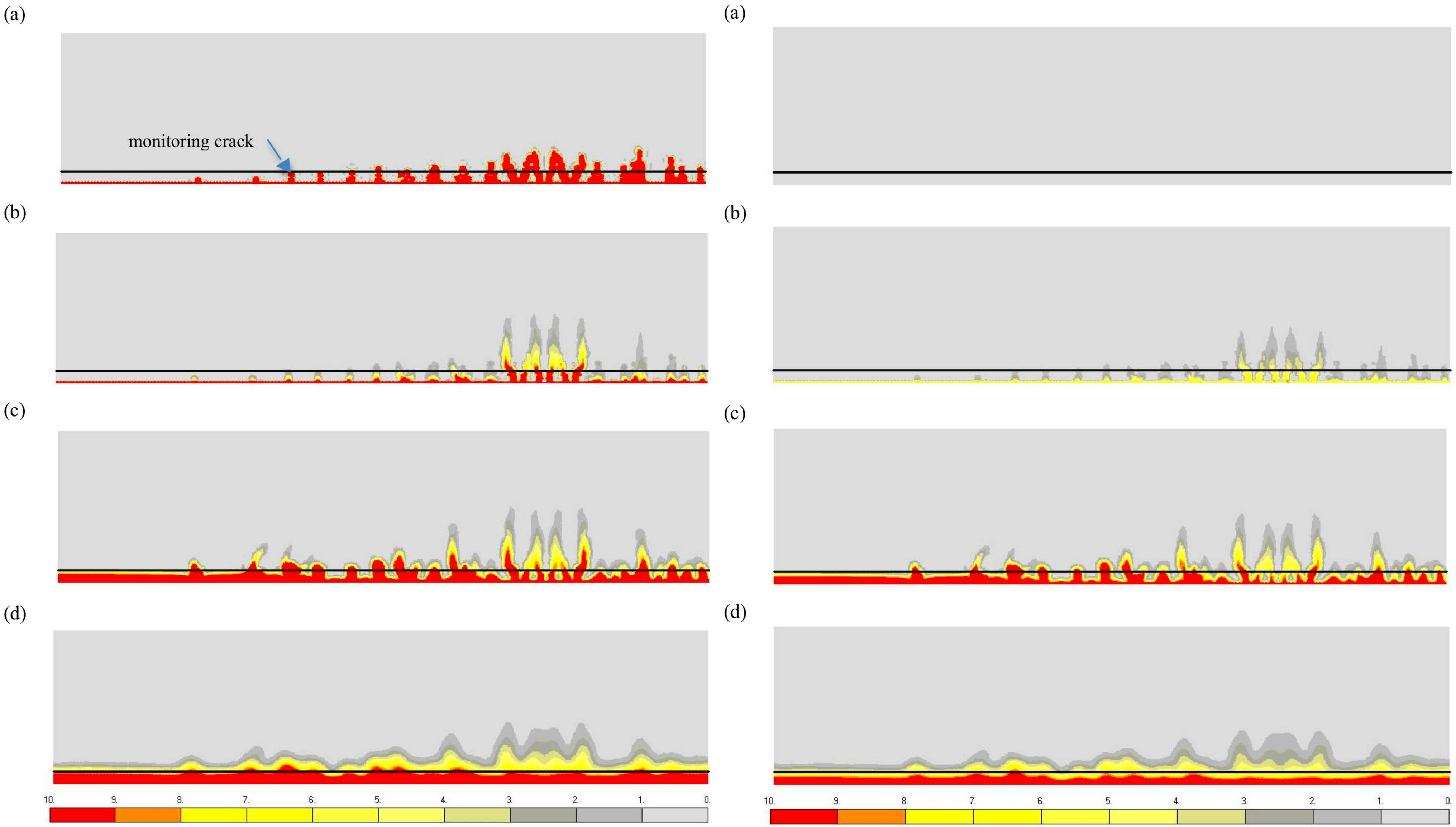

- Immediately after crack opening, water and free chlorides penetrate into the crack
- In good agreement with experimental observation (Wittmann et al. 2009; Marsavina et al. 2008)

Distribution of free chlorides (red = 8 kg / m^3 of pore solution)

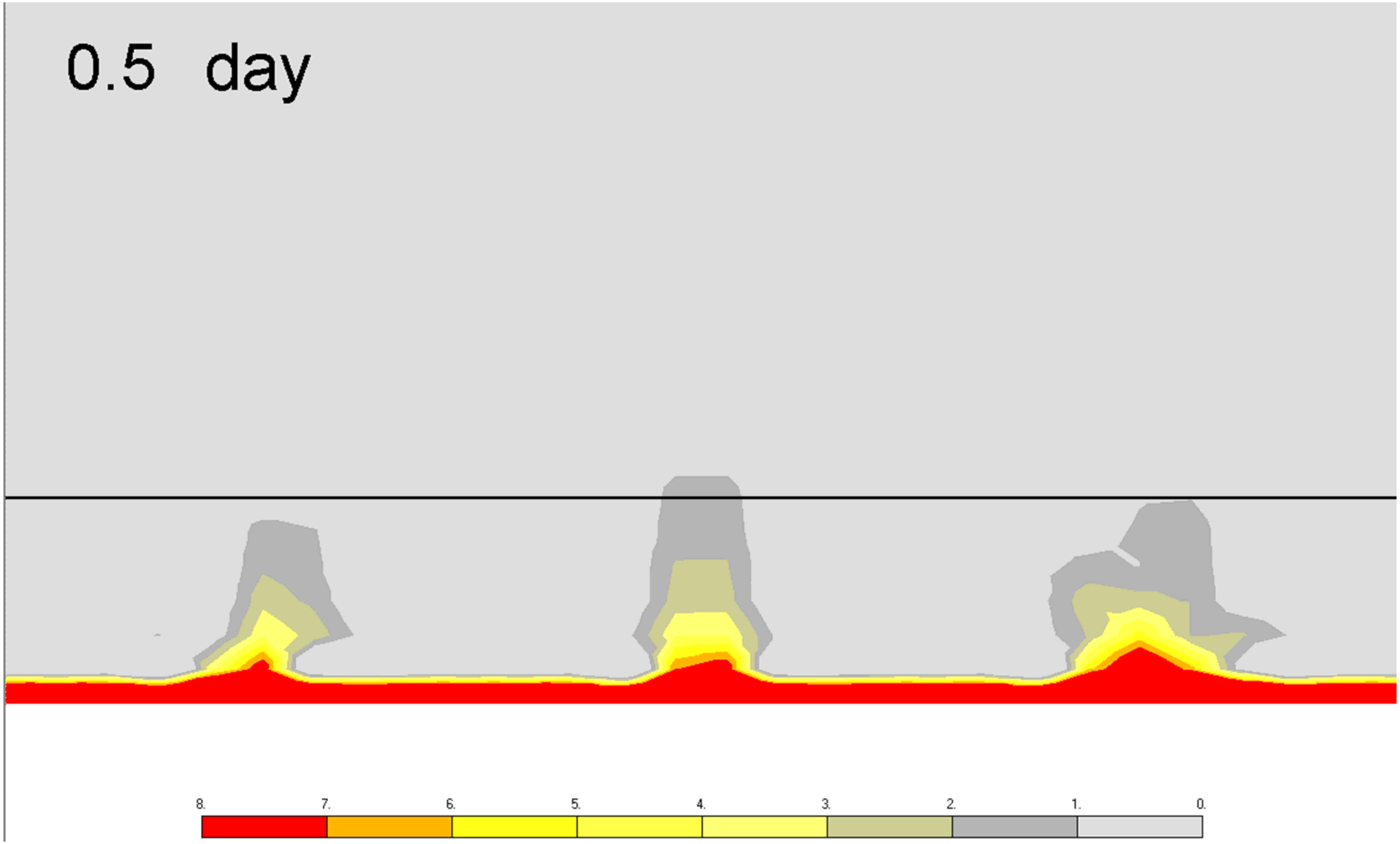

Distribution of free chlorides over the slab depth

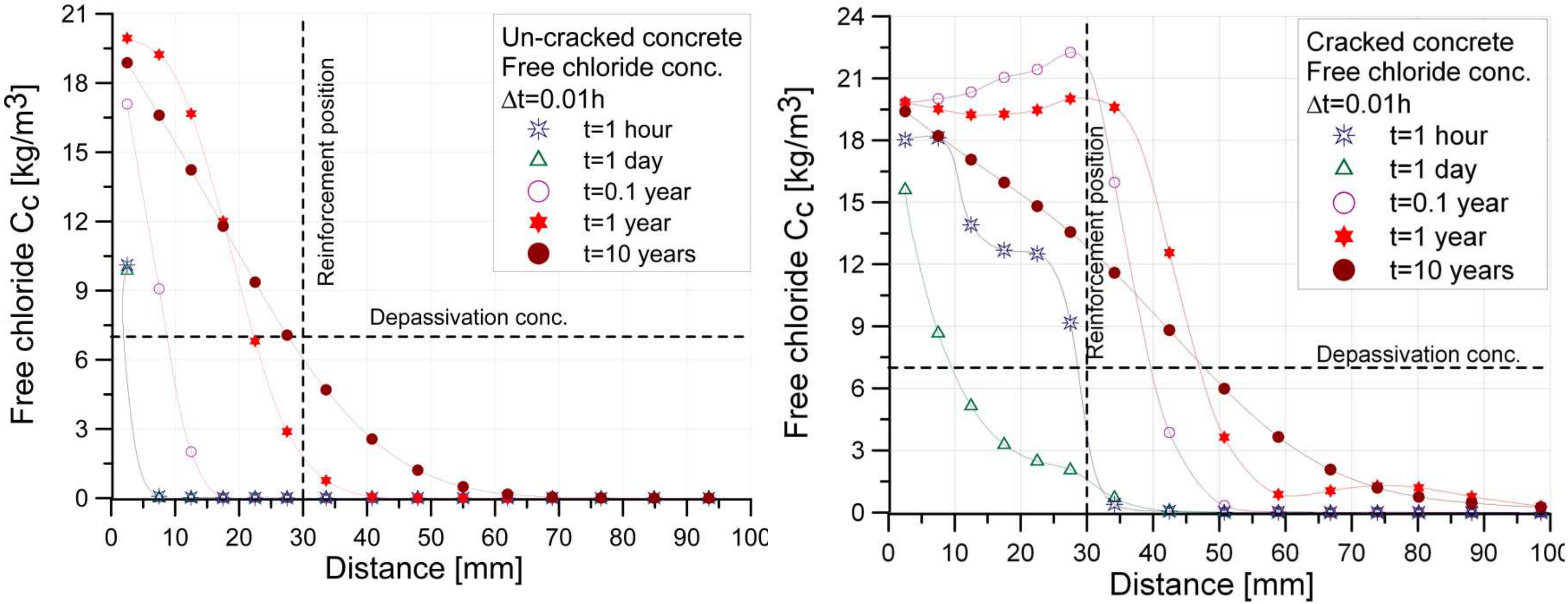

un-cracked

over the crack length

Distribution of free chlorides along reinforcement bar

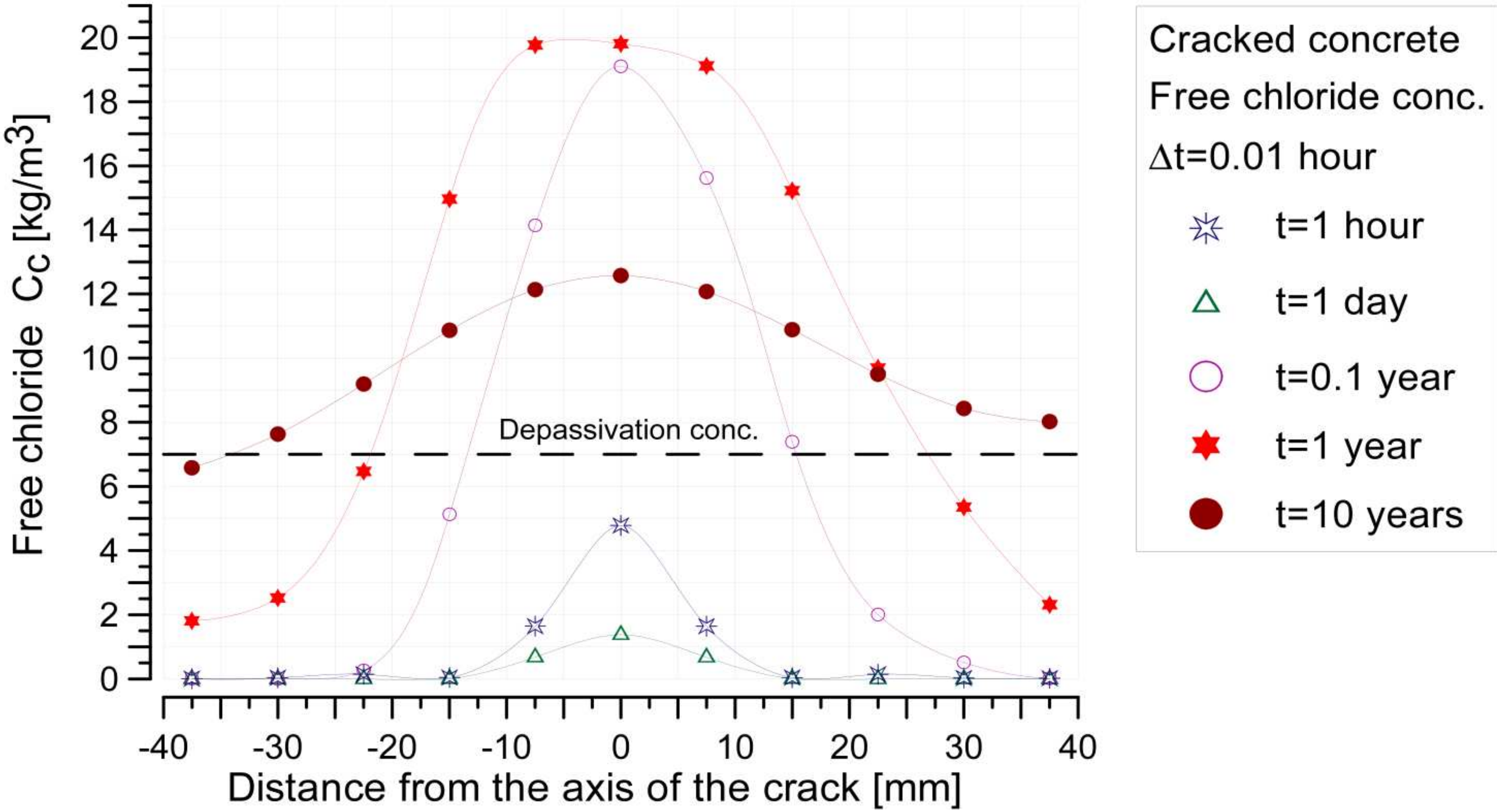

- After a certain time the free chlorides penetrate in the region between the cracks
- Also observed in experiments (Marsavina et al. 2008)

Numerical example (2)

(After depassivation of reinforcement)

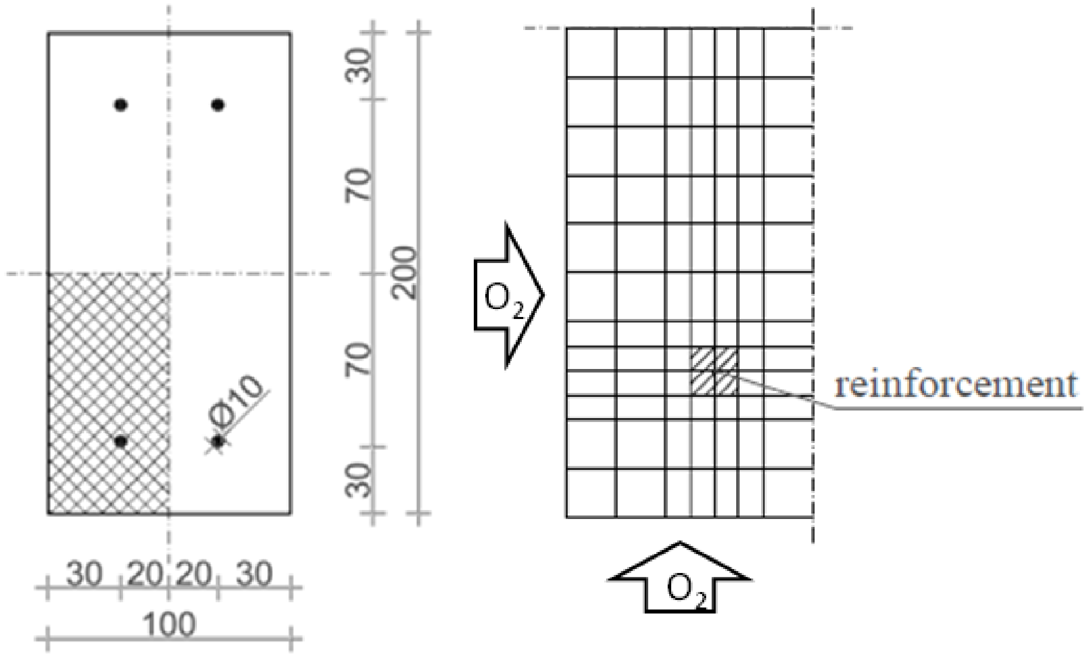

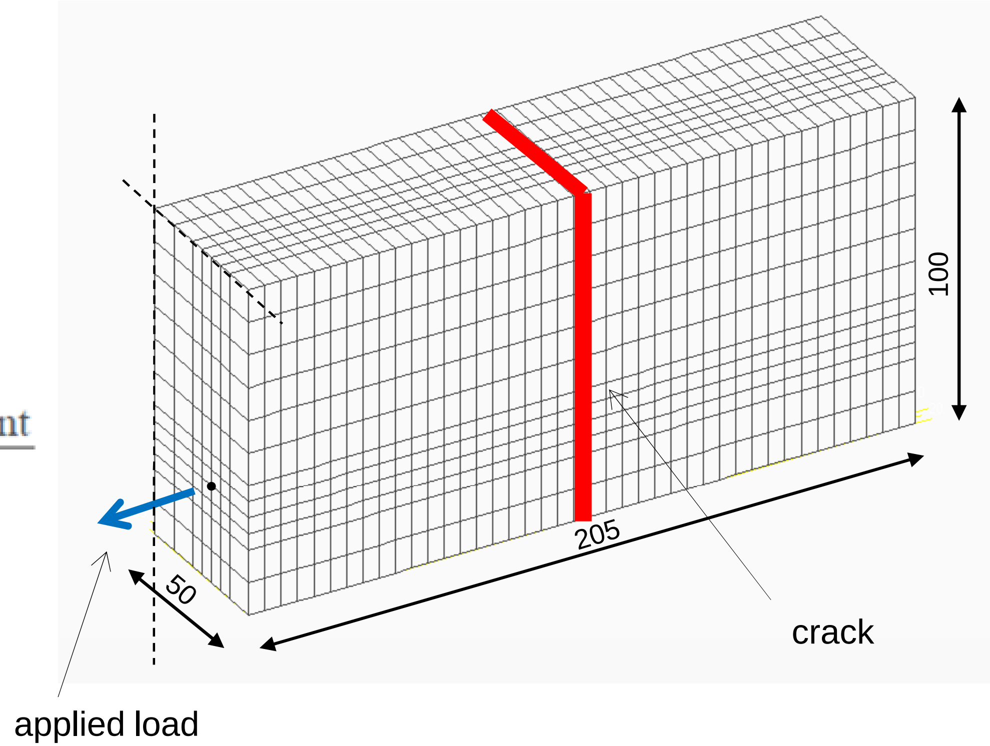

Investigated:

- Influence of concrete quality on corrosion rate
- Calculation of maximal corrosion rate as a function of concrete quality and saturation
- Influence of the crack (induced by external load) on corrosion rate
- Calculation of corrosion induced damage (CiD)
- Influence of the transport of rust on CiD

Assumptions:

- Analysis starts at t=0 (depassivation assumed)
- Saturation of concrete is constant

Ozbolt et al., 2011

Numerical example (2)
(After depassivation of reinforcement)

Parameters	Value
Faraday's constant, F (C/mol)	96486.7
Anodic exchange current density, i_{0a} (A/m^2)	1.875×10^{-4}
Cathodic exchange current density, i_{0c} (A/m^2)	6.25×10^{-6}
Anodic equilibrium potential, Φ_{0a} (V vs. SCE)	-0.780
Cathodic equilibrium potential, Φ_{0c} (V vs. SCE)	0.160
Tafel slope for anodic reaction, β_a (V)	0.06
Tafel slope for cathodic reaction, β_c (V)	0.160

	Saturation (%)	35	40	45	50	55	60	65	70	75	80	85	90	95
w/c =0.4	**Oxygen diffusivity, D_o (10^{-8} m^2/s)**	3.36	2.75	2.15	1.55	1.30	1.20	1.00	0.75	0.45	0.30	0.20	0.13	0.07
	Electrical conductivity, σ (10^{-3} Ω^{-1}m^{-1})	0.01	0.03	0.07	0.20	0.25	0.53	0.75	1.0	2.0	6.0	10.0	11.2	12.5
w/c =0.7	**Oxygen diffusivity, D_o (10^{-8} m^2/s)**	11.6	10.7	10.2	9.30	9.00	8.00	7.50	6.00	5.00	3.50	2.50	1.50	1.00
	Electrical conductivity, σ (10^{-3} Ω^{-1}m^{-1})	0.5	1.00	1.81	2.75	3.00	4.28	8.70	9.52	10.5	11.5	12.5	13.5	14.2

Distribution of oxygen for uncracked and cracked concrete

- Good quality concrete (w/c = 0.4)
- Saturation of 45%

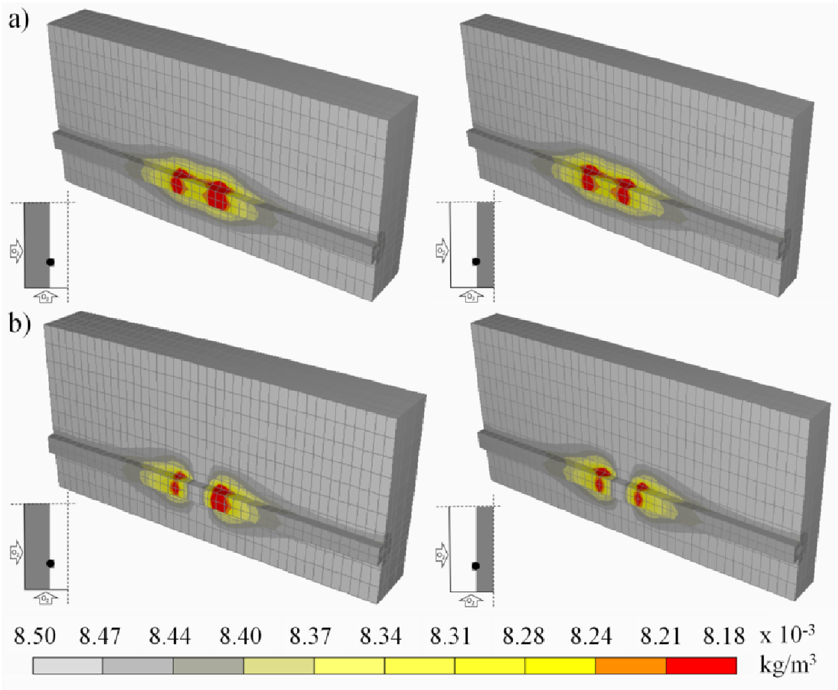

After 10 minutes after of corrosion process
a) Uncracked Concrete
b) Cracked concrete

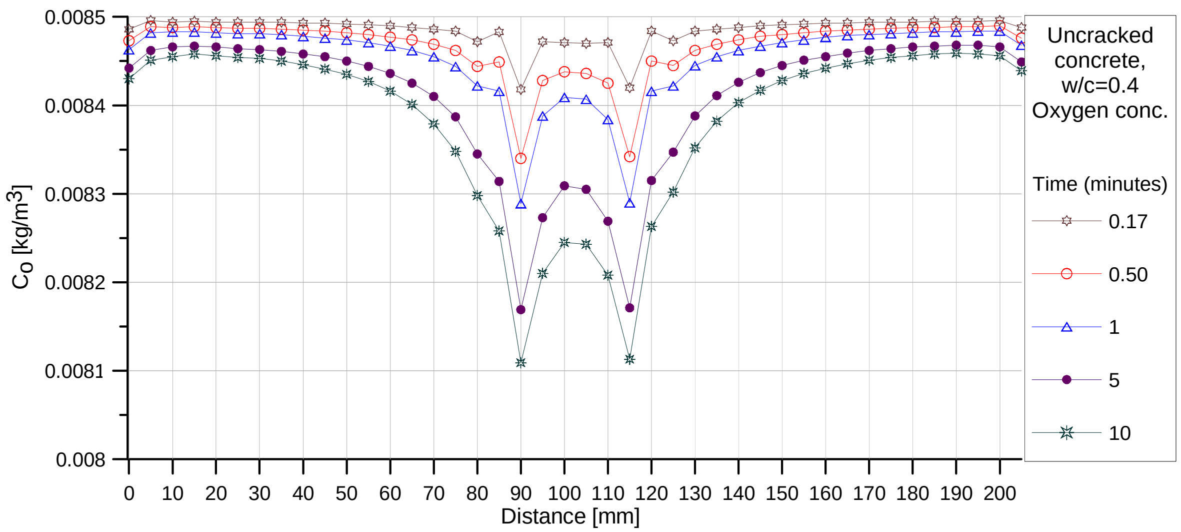

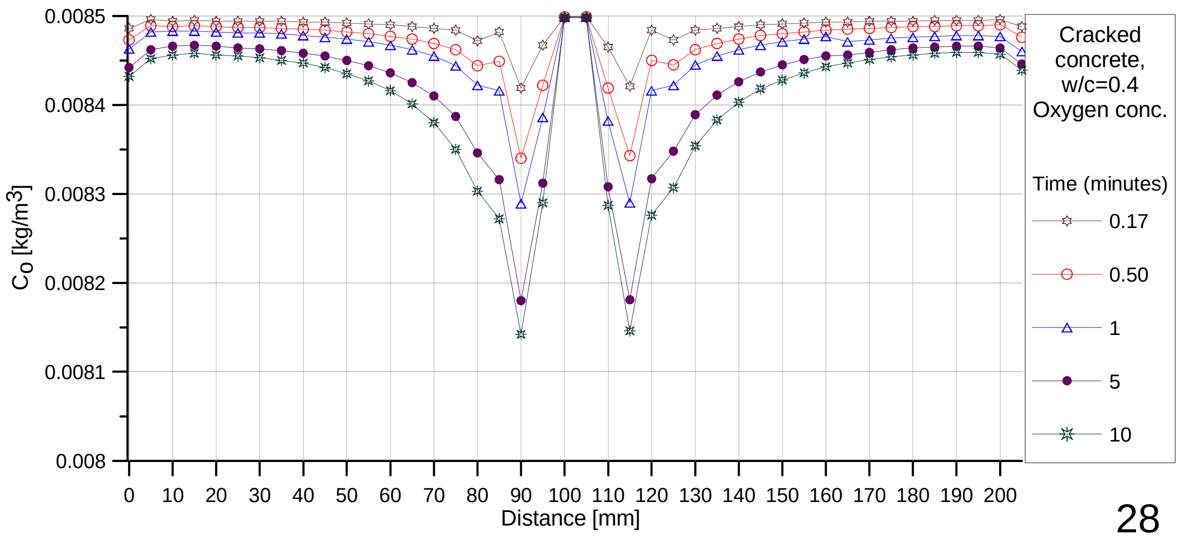

Distribution of corrosion current density for uncracked and cracked concrete

- Good quality concrete (w/c = 0.4)
- Saturation of 45%

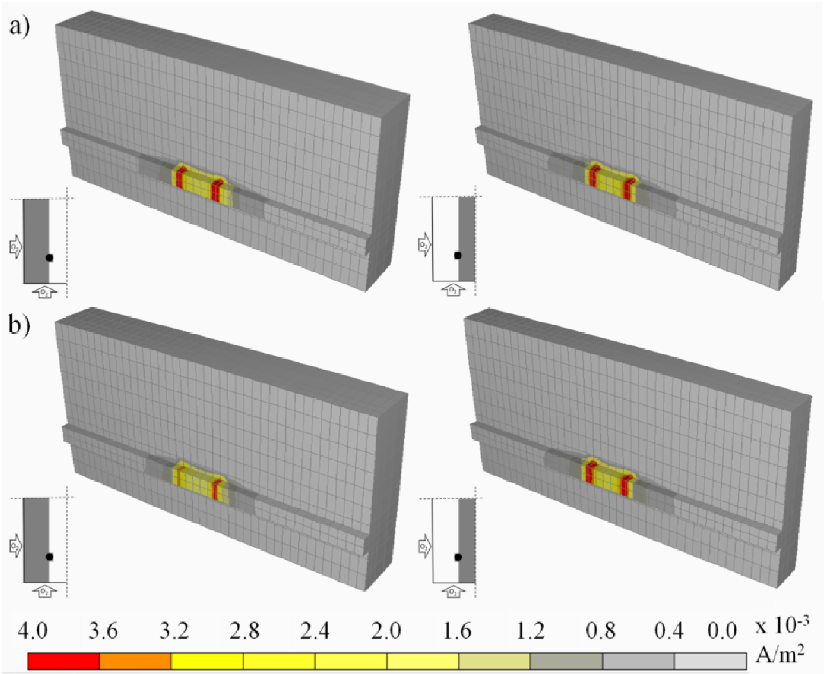

- The highest corrosion rate is obtained in the anode-cathode transition zone

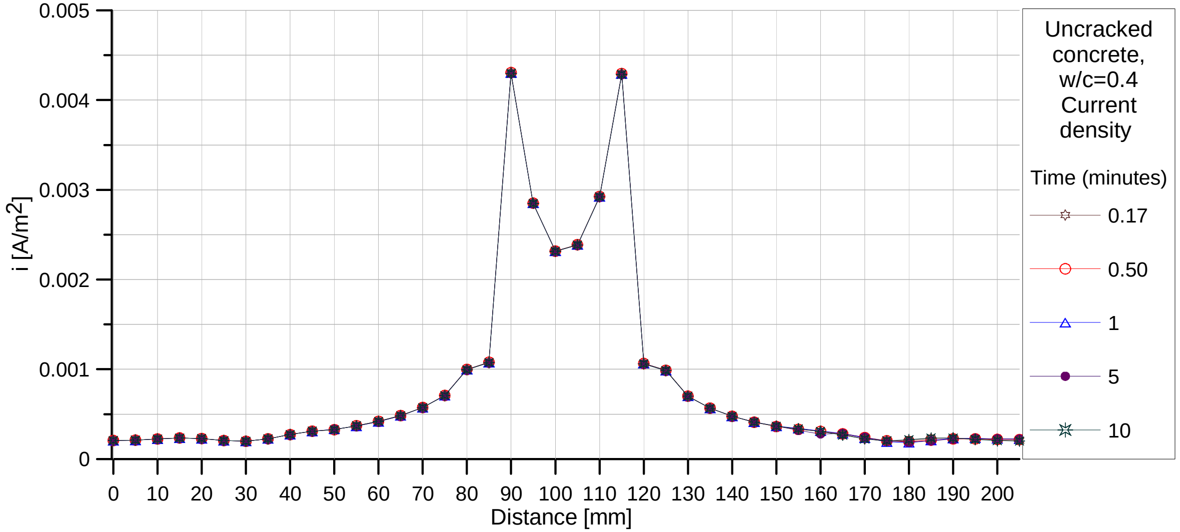

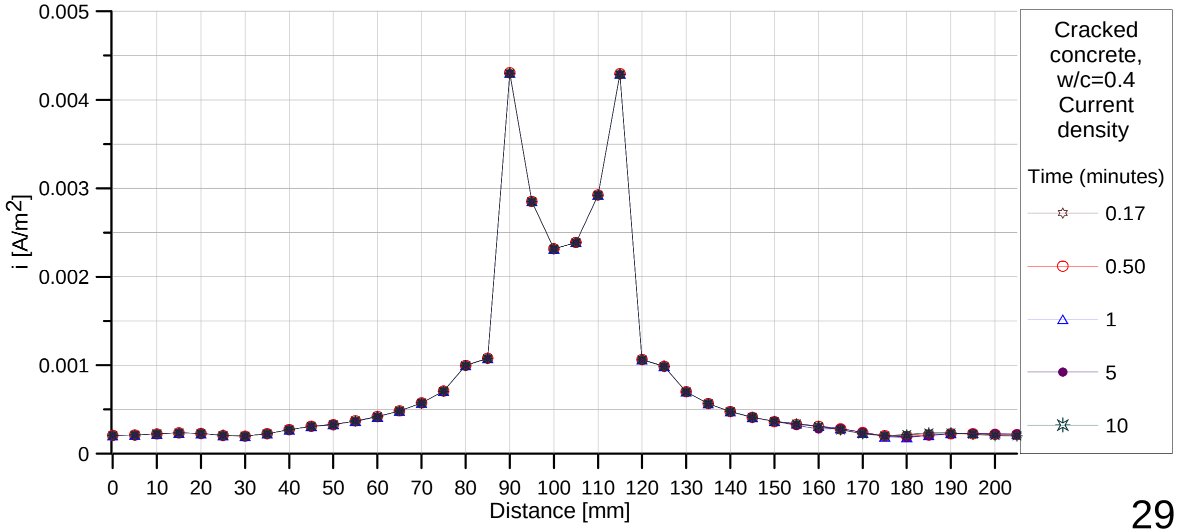

Relation between saturation and current density (corrosion rate)

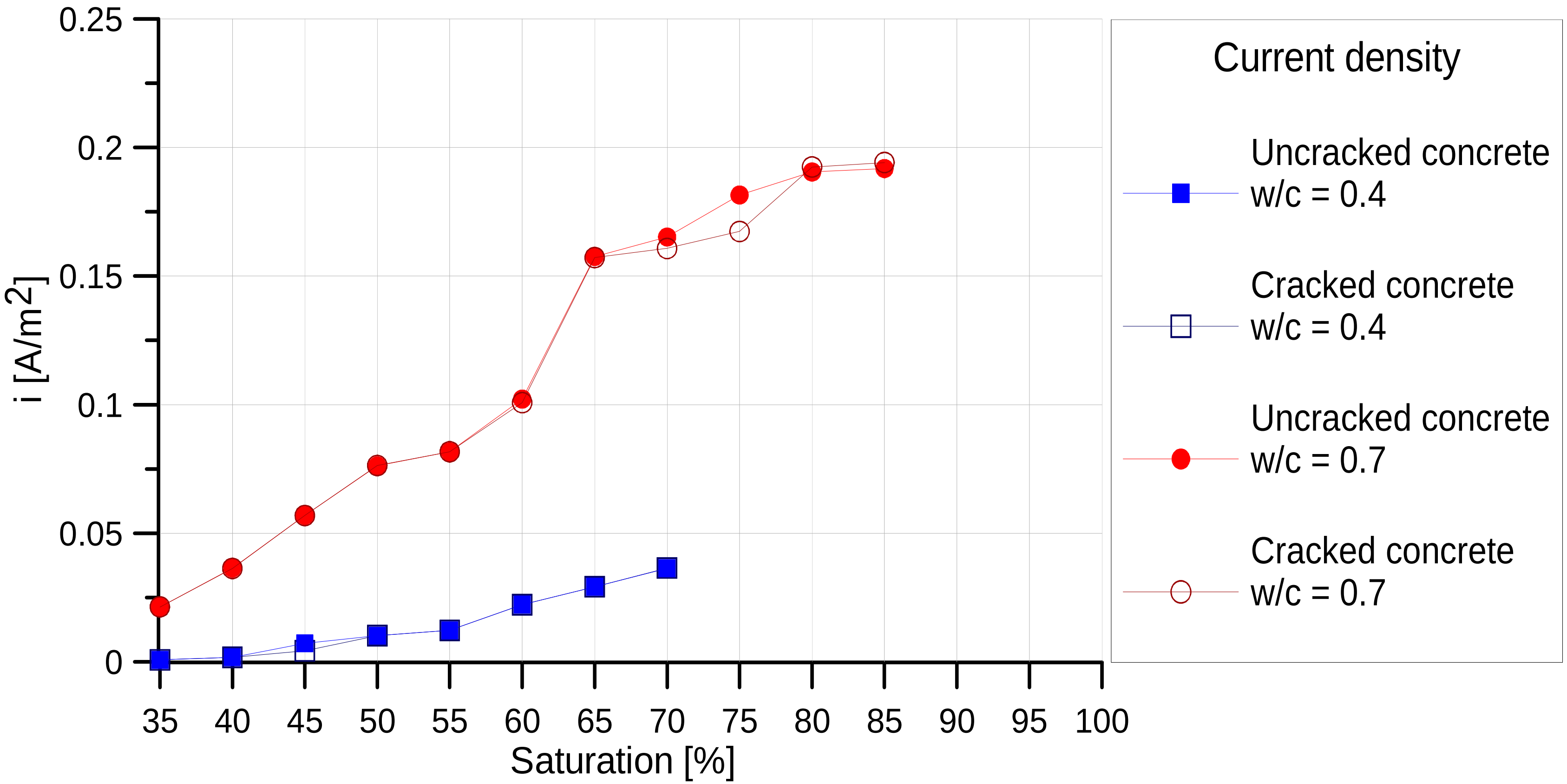

- Corrosion rate - higher in poor than in good quality concrete
- Maximal current density at critical saturation of:

  Good quality concrete → S=70%
  Poor quality concrete → S=85%

Relation between saturation and current density (corrosion rate)

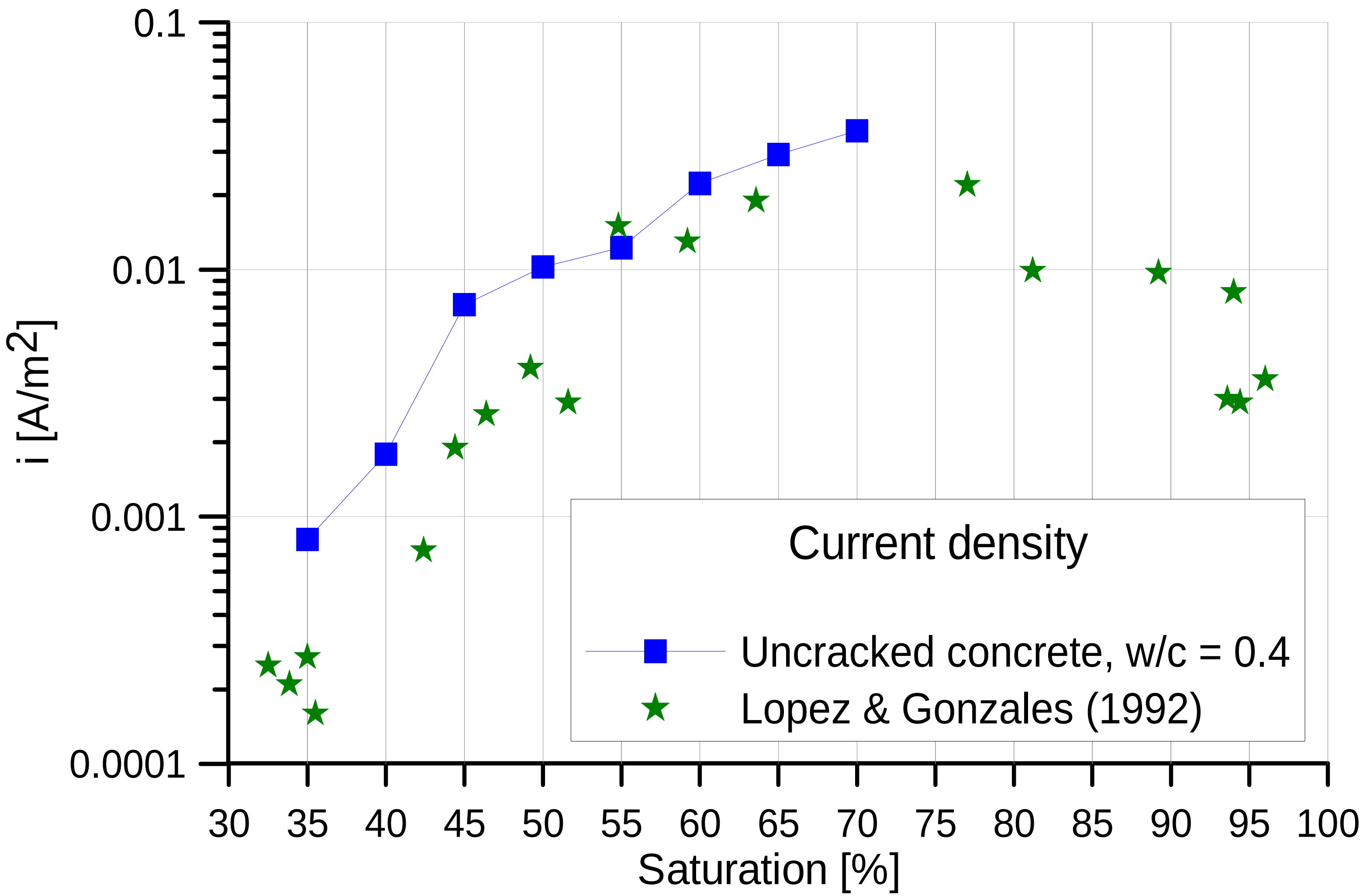

Corrosion induced damage (initially undamaged concrete, d=12 mm, saturation 55%)

Without transport of rust

1 YEAR

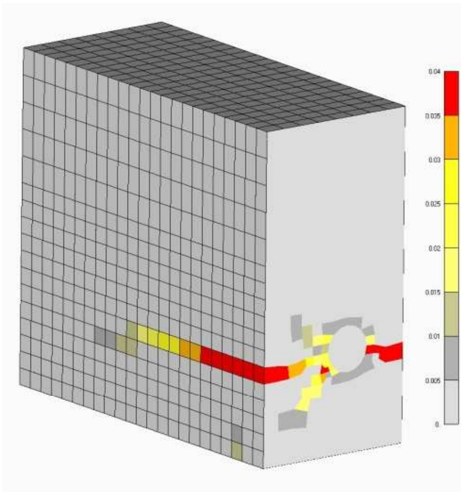

1.5 YEARS

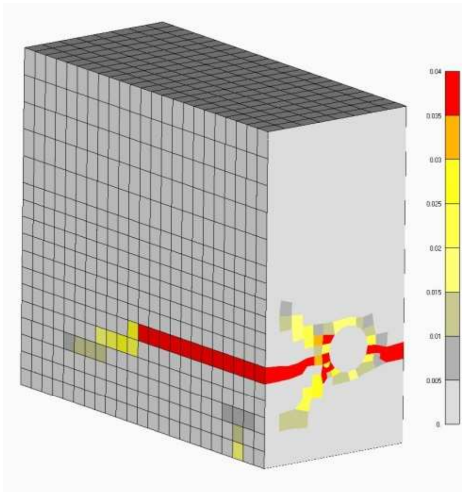

2 YEARS

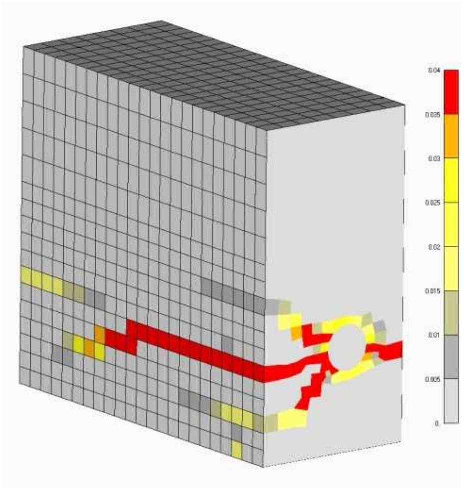

3 YEARS

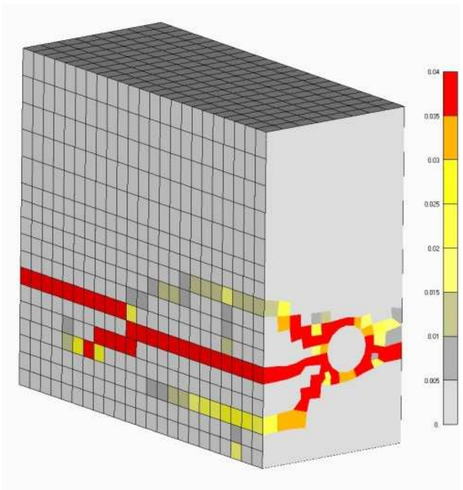

With transport of rust

1 YEAR

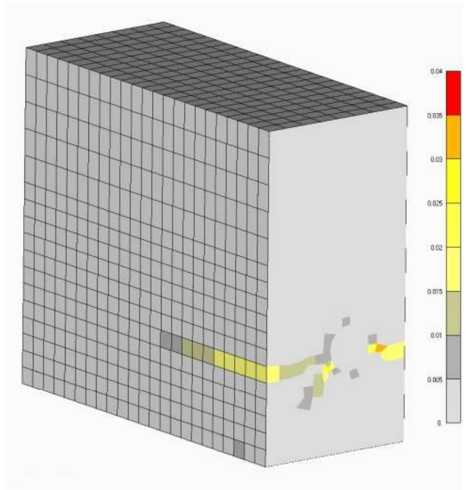

1.5 YEARS

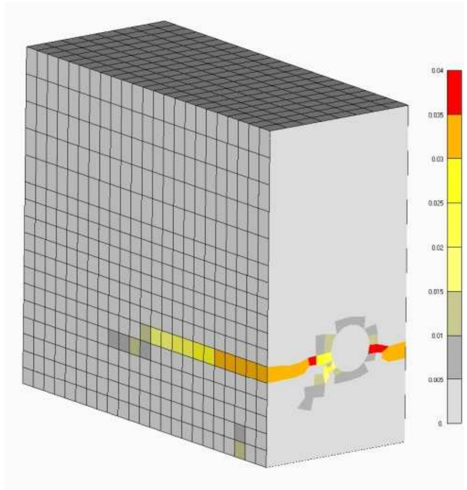

2 YEARS

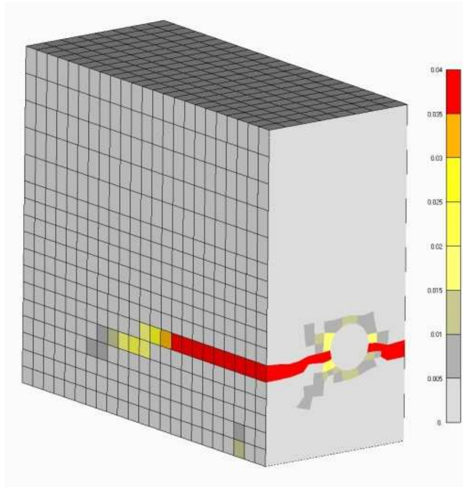

3 YEARS

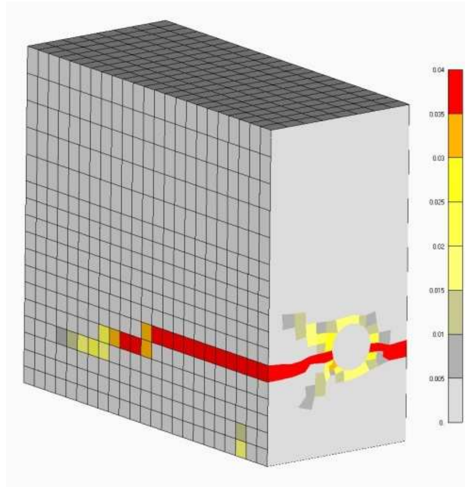

Relation between saturation and current density (corrosion rate)

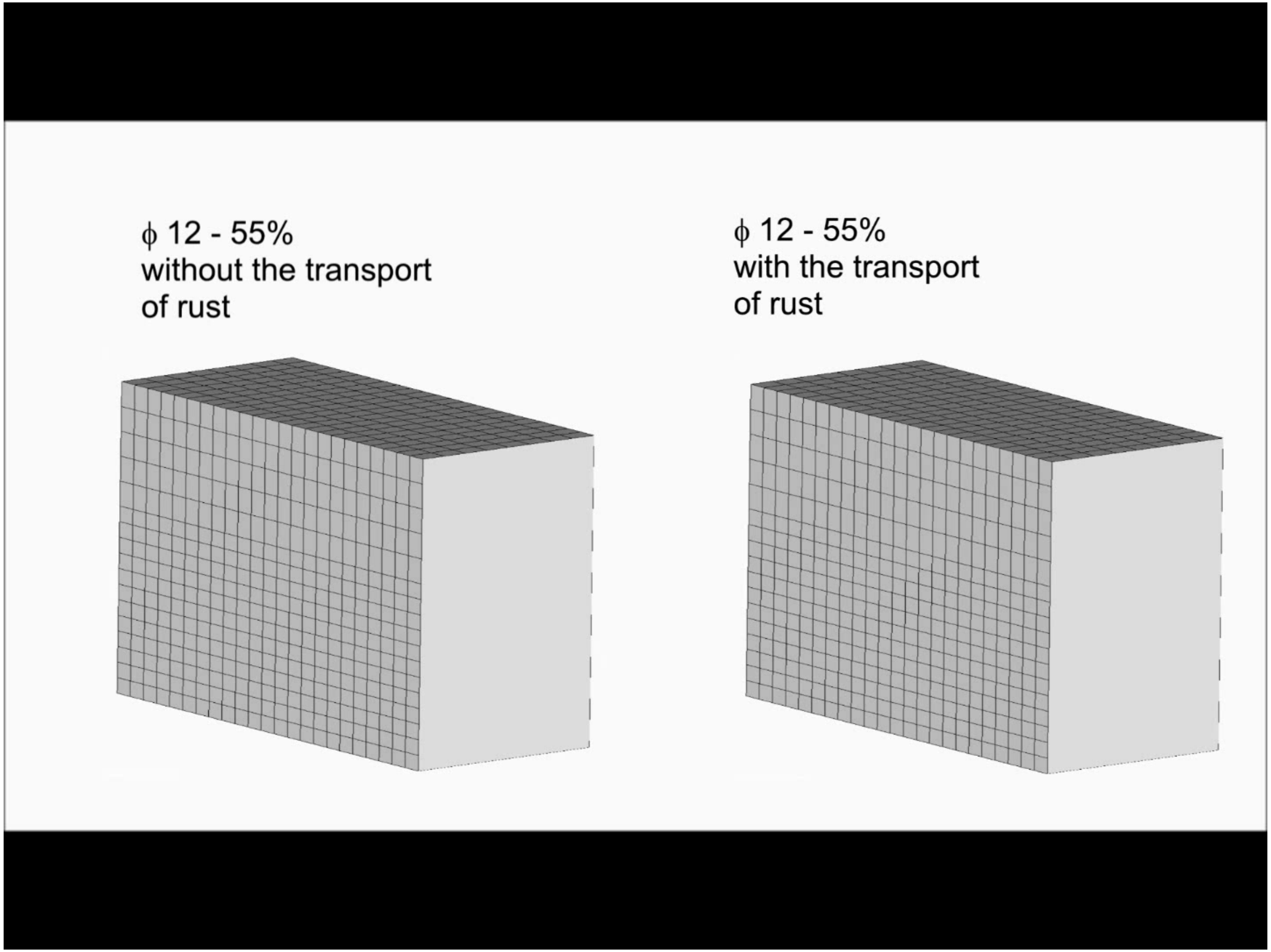

Damage after 3 years

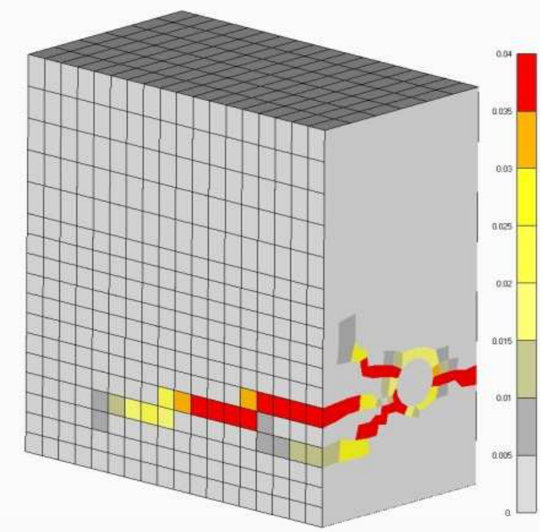

Rust distribution in the cracks after 3 years

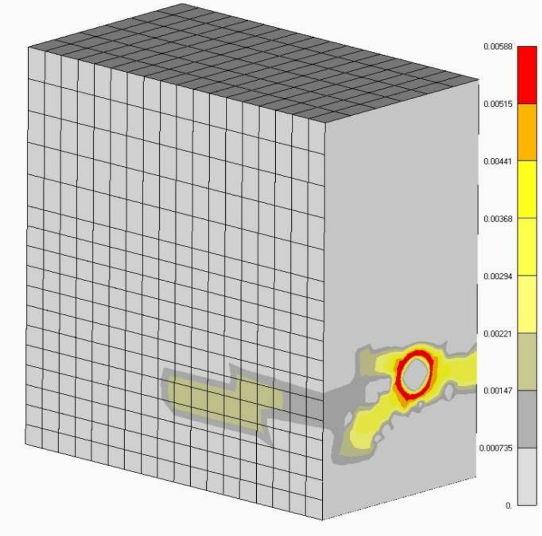

Oxygen distribution for $\phi 10$, 55% saturation, with the transport of rust

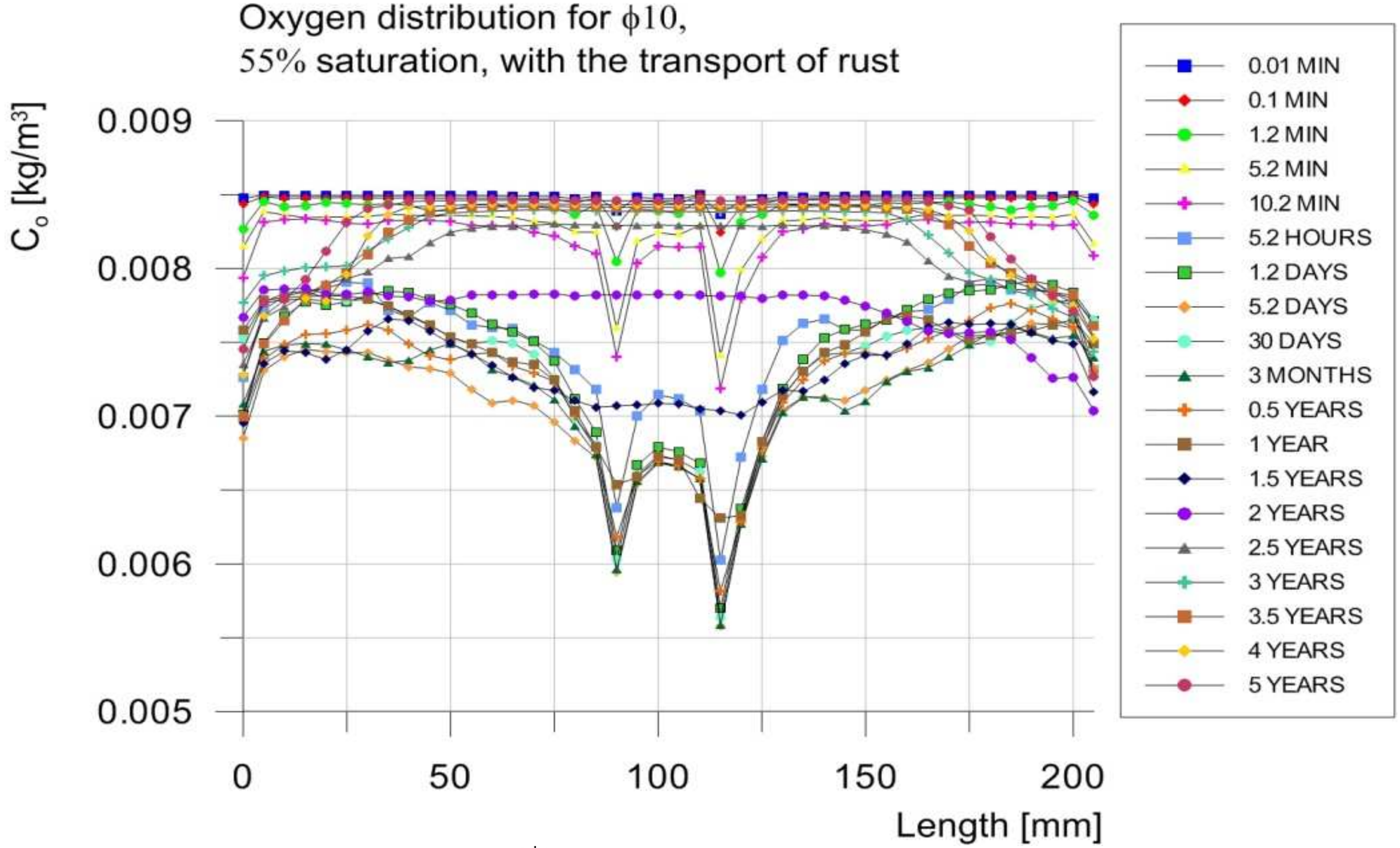

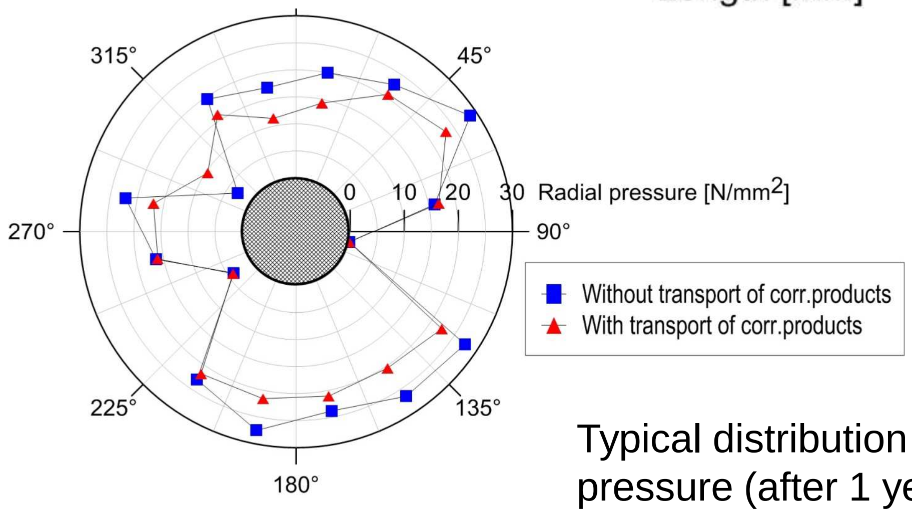

Typical distribution of radial pressure (after 1 year)

Consumption of oxygen in the anode-cathode transition zone
(d=12 mm, saturation 55%)

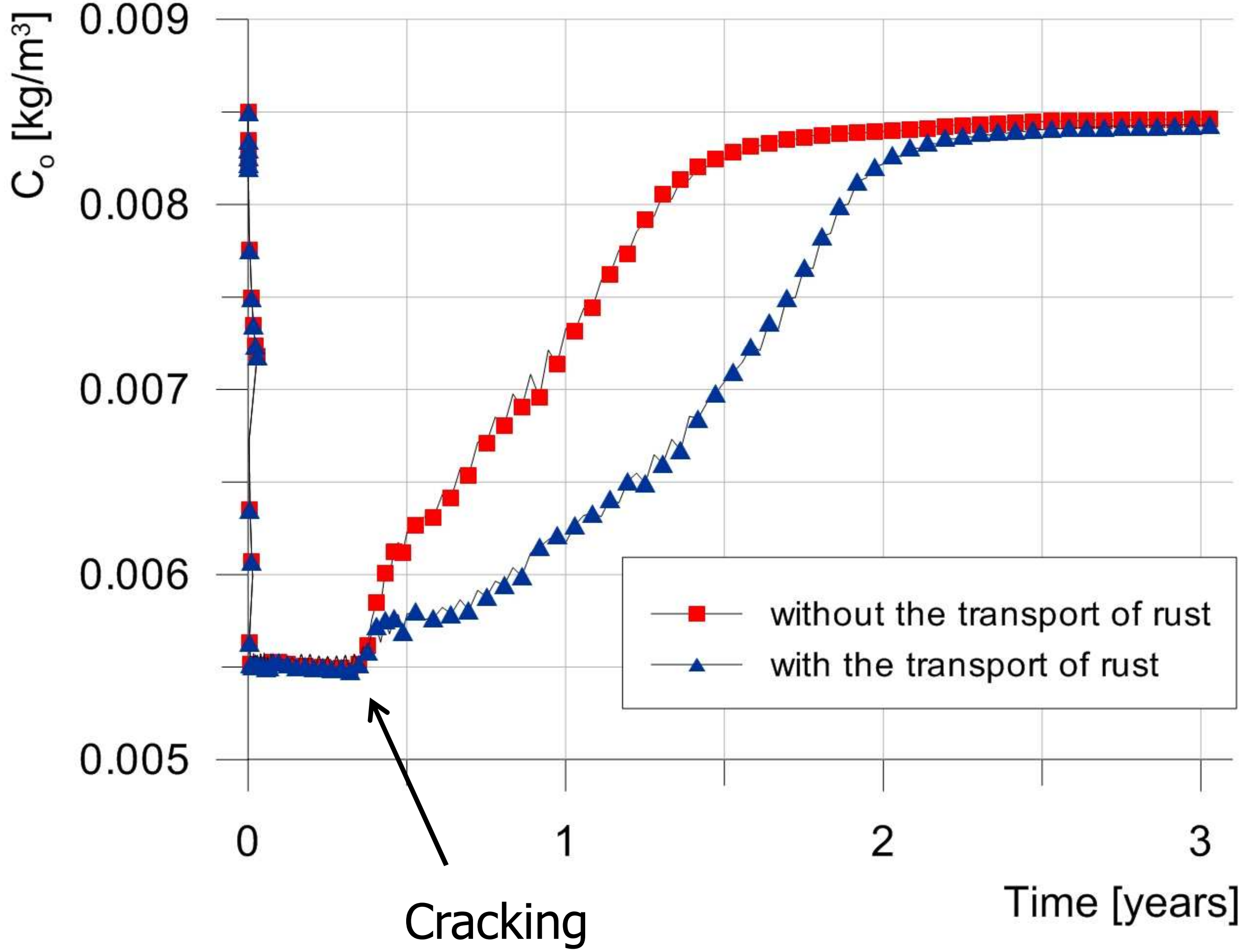

Summary and conclusions

- Fully coupled 3D chemo-hygro-thermo mechanical model for transient analysis of corrosion processes before and after depassivation of steel reinforcement in concrete is developed and implemented into 3D FE code
- The numerical results are in good agreement with the available experimental observations and with the results known from the literature
- Damage of concrete (crack) significantly reduces depassivation time, however, for assumed conditions (constant saturation) crack does not significantly influences corrosion rate
- Corrosion rate is much higher in poor (S=85%, i=0.194 A/m^2) than in good (S=70%, i=0.045 A/m^2) quality concrete
- Transport of rust through cracks reduces unfavorable effect of corrosion induced damage of concrete cover